AF TECHNICAL REPORT NO. 54-405 September 1954

FINAL REPORT

INVESTIGATION OF THE PRINCIPLE AND MECHANICS OF THERMAL CYCLIC ICE REMOVAL

Myron Tribus
Stuart W. Churchill
H. E. Stubbs
M. P. Moyle
Otto Reuhr
Joseph Rutkowski
T. J. Herrick
Paul Wing
J. A. Nichols

Engineering Research Institute, University of Michigan
Project No. 2128-7-F—Contract 33(600)-23549

United States Air Force
Air Materiel Command
Wright-Patterson Air Force Base, Dayton, Ohio

PREFACE

The work reported in this paper was done cooperatively by the Icing Research Staff of the Engineering Research Institute, University of Michigan. The program was initially supervised by Dr. Myron Tribus and later by Dr. Stuart W. Churchill and was under the technical direction of Mr. H. E. Stubbs. Dr. R. B. Morrison also had supervisory responsibilities.

The thermal analysis was done by M. P. Moyle and Otto Reuhr and the force analysis by Joseph Rutkowski, J. A. Nichols, and T. J. Herrick. Measurement of water thickness with the ice condenser was done by Paul Wing and experimental work by Roger Glass, A. E. Wood, Joseph O'Brien, and Frank Vogenitz.

SUMMARY

Thermal-cyclic ice removal from aircraft has been investigated theoretically and experimentally. The theoretical criteria for ice removal were generally confimed by the experimental work. The procedure developed for predicting whether ice will be removed by a given heating cycle under any given meteorological conditions can be outlined as follows:

1. Calculate the removal pressure from the velocity of the aircraft and the aerodynamic characteristics of the aerofoil. The removal pressure is the difference between the stagnation pressure and the average pressure on the ice. The average pressure on the ice may be approximated moderately well by taking the pressure distribution over the clean airfoil.

2. Calculate the equilibrium temperature of the ice as given by Messinger (Reference 6).

3. Calculate the thickness of water that will be melted from the ice temperature, the heating rate, and the time the heat is on (Eq. 5).

4. Calculate the retaining pressure on the ice from the water thickness (Eq. 11).

5. If the removal pressure is greater than the retaining pressure, the ice may be expected to come off.

TABLE OF CONTENTS

NOMENCLATURE

c = Heat capacity of solid.

L = Heat of fusion of solid.

U_o = Melting point relative to initial temperature of solid.

t_o = time for ice to rise to melting point.

K = Thermal conductivity of ice.

ϕ = Heat flux per unit area supplied by liter.

ρ = Density of ice.

X = Thickness of ice melted.

t = Time after melting starts.

F = "Function of" or force

$\sigma = \dfrac{\rho L X}{\phi t_o}$

$W = \dfrac{\rho_{ice}}{\rho_{water}} X$ = thickness of water layer formed on melting.

α = Thermal diffusivity.

$\beta = \dfrac{\phi^2 t}{\rho_w^2 L^2 \alpha_w}$.

a = distance, length.

U = Temperature.

P = Pressure.

γ = Surface tension constant.

R = Radius of curvature.

μ = Viscosity.

A = Area.

b = Width of ice.

$T = \left(\dfrac{\mu A b^2 \rho^2 L^2}{F \phi^2} \right)^{1/3}$

$B = \frac{W}{k}$.

$k = \left(\frac{\mu A b^2 \phi}{2F\rho L}\right)^{1/3}$

$S = \frac{2}{\pi}\left[\left(1 + \frac{t}{t_o}\right) \tan^{-1}(t/t_o)^{1/2} - (t/t_o)^{1/2}\right]$.

$Q = \frac{S}{t/t_o}$.

C = Electrical or thermal capacitance.

R = Resistance.

ϵ = Dielectric coefficient.

SECTION I

INTRODUCTION

Although thermal anti-icing systems which operate by keeping the aircraft structure clear of ice at all times have proved effective in protecting aircraft against icing conditions and permitting them to fly in all weather, such systems have high power requirements. In contrast, cyclic deicing systems, in which ice is permitted to accumulate on the aircraft surfaces for a period of time and is then removed by melting the interfacial bond between the ice and the aircraft surface so that the ice will be blown off by the aerodynamic forces, offer the possibility of much lower power consumption than an anti-icing system. It should be noted at the outset that the aerodynamic performance of an aircraft protected by deicing equipment will be inferior to an aircraft protected by anti-icing equipment since the aerodynamic surfaces will be covered most of the time during icing conditions by a thin coating of ice, whereas with an anti-icing system the aerodynamic surfaces are kept clean at all times. However, the total power the aircraft required to perform at a given speed and rate of climb is a better criterion for the effectiveness of an ice-protection system. The significant effects on this total power caused by ice-protection equipment are the power required to carry the weight of the protective equipment, the power required to operate the equipment, and the added power required by the aircraft because of increased drag and weight due to ice adhering to the aircraft. Although anti-icing systems require no power to overcome increased drag, it may well be that deicing systems compare favorably by the test of total power consumption. (In comparing different systems, it is of course assumed that both systems meet the primary requirements for keeping the aircraft airworthy and capable of pilot control at all times.) The purpose of this investigation was to determine the principles of thermal deicing so that they can be used in a rational design of aircraft ice-protection systems.

A qualitative picture of the ice-removal process can be obtained by considering a piece of ice attached to an aircraft surface that is protected by a thermal deicing system. The piece of ice is firmly attached to the aircraft surface by a solid bond, the exact nature of which is not necessary to examine for the present problem. It is sufficient to realize that even a small area of the solid bond will be strong enough to hold a piece of ice to an aircraft structure. Suppose now that the heating apparatus is turned on. The temperature of the ice and the structure to which it adheres will rise until some part of the ice comes to its melting point. Then as heating continues the ice will begin to melt and the heating process will be altered by the absorption of the heat of fusion. Since the heat source is inside the aircraft surface, the ice will always begin to melt at the ice-metal interface. As long as some parts of the solid bond remain intact, however, the ice will remain firmly in place. Finally, all the solid bond between the ice and the metal will be melted and the ice will be free to move under the influence of the forces acting on it. These forces are first, the aerodynamic forces from the air stream passing over the outside surface of the ice, second, the hydrodynamic forces in the water layer lying between the ice and the structure, and third, the force

of gravity on the ice. It cannot be assumed that the ice will immediately fly away from the aircraft as a result of these forces. Other possibilities that must be considered are that the ice will slide back along the surface, or that it will shift only slightly and find an equilibrium position in which it is more or less floating on the film of water. This phenomenon is possible because the surface tension forces existing in a thin film of water may be sufficient to counterbalance any aerodynamic forces tending to remove the ice. If the ice does not fly off from the aircraft surface immediately upon destruction of the solid bond, the influx of heat continues to melt additional ice, and the water film between the ice and the metal grows thicker, causing the forces of interfacial tension to change. Eventually the forces of the airstream will no longer be counterbalanced and the piece of ice will be swept away from the structure. The picture outlined above may be complicated by water which melts upstream, flows back, and refreezes. The details of the process described above thus depend on a number of parameters and the central problem of this investigation is to obtain a more precise and quantitative description of the process.

SECTION II

THE GENERAL PLAN OF THE INVESTIGATION

The parameters which are important in thermal-cyclic deicing may be grouped in several general categories. The first is the meteorological conditions. This category will include air temperature, liquid water content, drop size distribution, and air density. The second category pertains to the design and the performance of the aircraft and includes the geometry of the aircraft surface and the velocity of flight. A third category concerns the specifications of the ice-protection equipment and in the case of thermal-cyclic-deicing systems involves the distribution and strength of heating sources. The primary problem of this investigation was to determine under what conditions a piece of ice would be removed from the aircraft surface in question.

Decomposition of the overall problem into a number of simpler component problems is of considerable assistance in determining the criterion for ice removal. A method for doing this is shown schematically in Fig. 1. Considering the lower part of Fig. 1 first, it is supposed that a piece of ice will be removed when there is an unbalance of forces acting on it so that it will be accelerated relative to the aircraft structure. The forces on the piece of ice will arise first from the aerodynamic forces associated with the movement of air over the outside surface of the ice, and second, from the pressure distribution in the film of melted ice which lies between the ice and the aircraft structure. The forces in the water layer will depend on the thickness of the water layer, the motion, if any, of the water, and the amount of water surrounding the ice but not under it. The water thickness will in turn depend primarily on the method and rate of heating the ice and on the initial ice temperature. The equilibrium ice temperature is determined primarily by the rate of impingement of water, the flight velocity, and the air temperature. The rate of impingement of water is determined by the flight velocity, the water content and drop size of the clouds, and the geometry of the wing or other aircraft

surfaces. The aerodynamic forces acting on the ice will be determined by the shape of the ice and the wing and by the density and velocity of the airstream. Thus, in Fig. 1 the variables appropriate to the cyclic-thermal-deicing problem appear at the top. Below them appear a number of boxes, each of which represents the relationship between several of the primary variables. The new parameters in the boxes are in turn used in further analyses until it is possible to determine the criteria for the removal of the ice.

Several of the component problems represented by the boxes in Fig. 1 have already received attention by other investigators and been at least partially solved. The determination of the rate of impingement of water drops from their trajectories has received attention from Langmuir and Blodgett[5] and many others.[10] The methods of Langmuir and Blodgett have been mechanized by Tribus and Rauch and somewhat simplified by Tribus, Sherman, and Klein.[8] The determination of the equilibrium ice temperature has been given by Messinger[6]. This leaves the determination of the thickness of water film as a function of time, the determination of the aerodynamic forces on the outside of the ice, and the synthesis of the results as the major problems which must be solved before the dynamic behavior of the ice can be described and predicted. It is to these three problems that the attention of this present study is primarily directed.

SECTION III

THE LOCATION OF THE HEAT SOURCES

A thermal-deicing system gives promise of providing ice protection with less energy than an anti-icing system only if it expends nearly all the energy in melting the bond between the ice and the aircraft structure and very little in melting or vaporizing ice elsewhere or in heating the airstream. In order to avoid wasting heat, the icing system must heat the ice immediately adjacent to the structure rapidly so that its temperature will rise above freezing before large quantities of heat flow outwards into the airstream. The system must also avoid expending large quantities of heat in raising the temperature of the structure. It is also desirable that an aircraft surface protected by a deicing system cool rapidly, since any water which impinges on the surface after the ice has come off, but before the surface has cooled below the freezing point, will run back and freeze aft.

A heat source consisting of ducts carrying hot gases, such as are used in many anti-icing systems, has serious disadvantages when used in a deicing system. On any particular cycle it will be necessary to heat the ducts and the metal skin of the aircraft to rather high temperatures before the ice will begin to melt. After the heat is turned off, the thermal energy which has been stored in the metal skin will be conducted outward and prevent the surface from cooling rapidly. Thus a deicing system which uses hot gases will require considerably more energy and will have more difficulty with runback. These objections to a duct system become even more important in the new aircraft which use thicker skin and structural members. Furthermore, it is anticipated that some of the future aircraft will be designed with movable sections in the front parts of the wings. With such design it will be very difficult to construct ducting to distribute hot gas to the leading edges of the wings.

In contrast to the difficulties inherent in the use of ducting for cyclic deicing, electrical heating appears to offer a much more suitable method for the distribution of energy to accomplish the removal of ice. Wires can easily be run through movable sections and it is possible to generate heat in a resistance element on the outer surface of the aircraft structure just where it will be most effective in melting the bond between the metal and the ice without wasting energy elsewhere. In view of these advantages, it appears that deicing systems should use electrical power as their source of heat and the present study primarily considers such systems.

One method which has been used to produce heat in a deicing system is to embed electrical resistance wires in a boot of neoprene which is then cemented to the surface to be protected. The wires are positioned in the boot so that more neoprene is below them than above them. Since the neoprene is a good insulator, it impedes the flow of heat into the air frame. At the same time, but to a lesser degree, it impedes the flow of heat to the icecap and causes rather high wire temperatures to develop during operation of the heater. When the heating wires are turned on, the surface of the boot is not heated uniformly. There are hot spots over the wires and relatively cold regions in between them. This nonuniformity of surface temperature wastes heat because an excess of water is melted over the hot spots before the cold spots are melted at all. The excess water is also undesirable, since it runs back and freezes aft. An investigation was undertaken of the temperature variations which occur in a deicing boot under normal operation to see if they were large enough to be an important factor in the deicing process. The construction and dimensions of the heater boot are shown in Fig. 2. The thermal transients in the boot were analyzed by dividing a section of the boots into thirteen cells and writing difference equations between the cells approximating the differential equations which actually govern the heat flow. The equations were then solved on a differential analyzer. The method of dividing a section of the boot into cells is shown in Fig. 3 and superimposed on the picture is a diagram of the thermal network. The derivation of the equations is given in Appendix A.

Figure 4 shows the temperatures in different cells as a function of time in a typical run on the differential analyzer. The heaters were energized for thirty seconds and the temperature in the icecap rose about 60°F during the cycle. The difference in temperature between Cell No. 4, which is directly over the heating element, and Cell No. 6, which lies midway between heating elements, is plotted in Fig. 5. It can be seen that the temperature difference is greater than 20°F through a large part of the heating cycle. Since the calculation method is rather crude (because the division into cells is coarse), the numerical value thus obtained cannot be relied on to much better than 20 percent. However, the results clearly indicate that sizable temperature variations can occur along the surface of a boot using wire heaters.

Further confirmation of this conclusion was obtained by making interferometer pictures of a thermal deicing boot of the same construction. For these pictures the boot was not covered by a layer of ice, but was cooled by free convection. In the photograph fringe shifts indicate temperature differences with each fringe being equivalent to approximately 8°F. Figure 6 is the interferogram of the boot two seconds after the power at seven watts per square inch had been turned on. There is one fringe shift between the hot and cold parts of the surface of the boot; indicating temperature variations of about 8°F. Figure 7 is an interferogram of

a boot in which the heating elements have twice as great a spacing, i.e., the structure is the same as shown in Fig. 2 except that the distance between heating elements is 0.1 inch. The interferogram is taken again two seconds after the boot is energized at seven watts per square inch. The fringe shift between hot and cold spots is two or perhaps a little more; indicating temperature variation of 16 to 18°F along the surface.

Thus both the computations on the differential analyzer and the interferometry studies indicate that considerable variations will occur in the surface temperature of a deicing boot using wire heaters as shown in Fig. 2. It is therefore desirable that deicing systems be built with a more uniformly distributed heat source. The ideal situation, of course, would be to have the heating element distributed uniformly over the whole outside of the aircraft surface that is to be protected.

SECTION IV

THE RATE OF MELTING OF ICE

The preceding sections have discussed the desirability of having a uniform heat source which is close to the surface of the structure. An analysis will be made in this section of the melting process in the ideal case in which heat is generated uniformly at the surface of the aircraft structure and no heat is conducted backward into the structure. This idealization can be realized to a fair approximation with certain designs of heater elements and the analysis will also serve as a basis for understanding the process of melting even in systems where the idealization is not so well realized. In order to simplify the mathematical treatment it will be further supposed that the icecap frozen to the structure is infinite. This supposition will not introduce a serious distortion in the results if the square of the ice thickness is greater than the product of the time of heating and the thermal diffusivity of ice. If this condition is not met convectiv heat transfer must be considered.

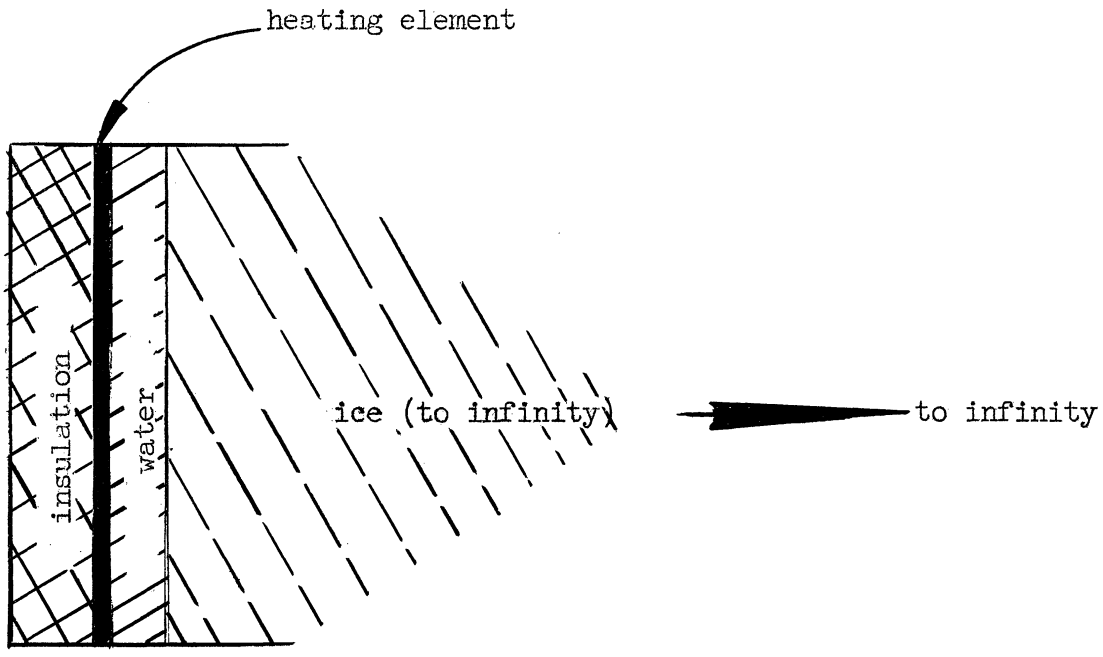

The idealized problem is shown on the preceding page. The heat generated per unit area by the heating element is a constant and all the heat is conducted to the right. For a short time after the heater is energized the only effect will be to raise the temperature of the ice. Soon, however, ice will begin to melt and there will be a water layer adjacent to the heating element. Beyond this, ice will extend to infinity. As time increases, the temperature increases in both the ice and water layer, more ice melts, and the thickness of the water layer increases.

For purposes of deicing, interest is primarily in the thickness of the water layer as a function of time and secondarily in the temperature throughout the system. The analysis of the melting process can be considerably simplified by considering the disposition of the electrical energy. Until melting starts, all the energy developed in the heating element goes to raising the temperature of the icecap. After melting starts, the energy goes to raising the temperature of the ice, raising the temperature of the water, and providing energy for the heat of fusion at the interface. Since in practical deicing systems the water layer involved will be quite thin, perhaps a few hundredths of an inch, the temperature difference across the water layer cannot be very large, even though the thermal gradient is quite high. The analysis of melting will therefore be simplified by neglecting energy expended in heating the water and supposing that all the heat flux generated in the heating element will appear at the ice-water interface and be expended either in melting ice or in raising the temperature of the ice. The error resulting from this assumption will be examined later.

An extensive study of the problem of melting solids as formulated was made by H. G. Landau.[4] Landau introduces two parameters into his analysis: m, which is proportional to the ratio of heat energy required to raise the temperature of a piece of ice to its melting point to the energy to melt it and is defined by

$$m = \frac{\sqrt{\pi}\, c\, U_o}{2\, L} \quad , \tag{1}$$

where c = the heat capacity of the solid,

L = the heat of fusion of the solid, and

U_o = the melting temperature of the solid relative to the initial temperature (U_o is thus positive);

and t_o, which is the time required for the ice immediately adjacent to the heater to rise to the melting point, i.e., the time in which the heater is on, but before melting starts. The value of t_o is

$$t_o = \frac{\pi}{4} \frac{K\, c\, \rho\, U_o^2}{\phi^2} \quad , \tag{2}$$

where K = thermal conductivity of ice,

ϕ = heat flux per unit area supplied by heater, and

ρ = density of ice.

With a change of notation and rearrangement Landau's results can then be expressed

$$(3) \qquad \left\{1 + 2/\sqrt{\pi}\, m\right\} \sigma = F\,(t/t_o,\ m),$$

where $$\sigma = \frac{\rho L X}{\phi t_o} = \frac{4}{\pi} \frac{\phi L}{K c U_o^2} X,$$

X = thickness of ice melted,

t = time after melting starts, and

F denotes "function of".

t is measured from the beginning of melting. The time from the initial application of power is $t_o + t$. For deicing the important quantity is thickness of the liquid layer formed rather than X, the thickness of the ice melted. The thickness of the liquid layer, W, can however be easily obtained by the relationship

$$(4) \qquad W = \frac{\text{density of ice}}{\text{density of water}} X .$$

For the special case $m = 0$, the differential equations become linear and it is possible to obtain the following analytical expression of the results.

$$(5) \qquad \sigma = \frac{2}{\pi}\left\{\left[(1 + t/t_o) \tan^{-1} (t/t_o)^{1/2}\right] - (t/t_o)^{1/2}\right\} .$$

The equation is plotted in Fig. 8.

The present investigators analyzed the melting problem for $m = 0$ before discovering Landau's work. Since this work has a viewpoint somewhat different from Landau's and gives certain details that Landau omits, it is presented in Appendix B.

For $m \neq 0$, the differential equations are nonlinear and Landau therefore used a digital computer to obtain solutions which he presents graphically. However, for ice at temperature above -40°F, which is the lowest temperature at which aircraft icing occurs, m does not exceed 0.2. For m less than 0.2 the values of σ do not differ from those for $m = 0$ by more than 10 percent, so that for practical design calculations Eq. 5 is sufficiently accurate.

A special case arises when $U_o = 0$, i.e., when the ice is initially at the melting point, for t_o and m also equal 0, and Eq. 5 becomes indeterminate. However, if Eq. 5 is multiplied by t_o, it becomes

$$(6) \qquad \frac{\rho L X}{\phi} = \frac{2}{\pi}\left\{\left[(t_o + t) \tan^{-1} (t/t_o)^{1/2}\right] - (t\, t_o)^{1/2}\right\} .$$

If t_o now becomes 0, this reduces to

$$(7) \qquad \frac{\rho L X}{\phi} = t,$$

indicating that the amount of ice melted is proportional to $(\phi \cdot t)$, the total energy supplied, which is of course to be expected since it has been assumed that the heat expended in raising the water temperature is negligible and when $U_o = 0$ no heat is required to raise the temperature of the ice.

When U_o is equal to 0, however, the melting problem is susceptible to a more exact treatment in which it is not necessary to neglect the energy expended in raising the water temperature. This problem is analyzed in Reference 3 and with a changed notation the results are

$$(8) \qquad W = \frac{\phi t}{\rho_w L}\left(1 - \frac{1}{2!}\beta + \frac{5}{3!}\beta^2 - \frac{51}{4!}\beta^3 + \frac{827}{5!}\beta^4 \ldots\right),$$

where W = thickness of water,

ρ_w = density of water,

$\beta = \dfrac{\phi^2 t}{\rho_w^2 L^2 \alpha_w}$, and

α_w = thermal diffusivity of water.

No method for calculating the residue of the infinite series resulting from using a finite number of terms is suggested by Evans, Isaacson, and McDonald in Reference 6, so that the practical applicability of Eq. 8 is somewhat doubtful. Settling aside the question of the accuracy obtained from any finite number of terms in the series, Eq. 8 can be compared with Landau's solution for $U_o = 0$ to obtain an idea of the error introduced by the more drastic mathematical assumptions needed to handle an arbitrary initial temperature. Comparison of Eqs. 7 and 8, and consideration of the relationship of Eq. 4 indicate that neglecting the heat required to raise the water temperature is equivalent to using only the first term of the series in Eq. 8. The second and subsequent terms of the power series may then be taken as a measure of the error in calculating water thickness.

$$(9) \qquad E = -\left\{-\frac{1}{2!}\beta + \frac{5}{3!}\beta^2 - \frac{51}{4!}\beta^3 + \frac{827}{5!}\beta^4 \ldots\right\} .$$

Taking typical values of the parameters

ϕ = 1.2 cal/cm^2

ρ_w = 1 g/cm^3

L = 80 cal/g

$$\alpha_w = 0.00144 \text{ cm}^2/\text{sec}$$

$$t = 1 \text{ sec}$$

E can be calculated as

$$E = 0.04 = 4\% \ .$$

It should be stressed that the error discussed above is only the limit of the error in Landau's problem when the initial distribution approaches zero.

A more practical method to account for the energy used in heating water which comes from melting is to consider the temperature gradient-heat flux-average temperature relations for the water layer at its maximum thickness, compute the energy required to reach this average temperature for the volume of water present, and spread this energy uniformly over the computed time interval as a correction of the heat flux. Although this procedure may not be conservative, the uncertainties involved are not so great as those involved in the estimation of some of the design conditions.

Equation 5 is rather abstract and recapitulation of its application to the problem of deicing aircraft appears worthwhile. The dimensionless quantity σ is obtained by multiplying the thickness of the ice melted by a number of parameters which describe the meteorological conditions and the design features of the deicing system, namely, the rate at which heat is generated, the physical properties of ice, and the equilibrium temperature of the ice. Therefore, for any particular design and particular icing condition σ is the measure of the thickness of ice melted. The thickness of water can be calculated by reference to Eq. 4. The expression on the right in Eq. 5 is a function of time together with certain parameters which again are determined by the design of the deicing system and the meteorological conditions. Thus, is essence, Eq. 5 gives the relationship between thickness of water layer and the time that the heaters are on for given conditions, design, and weather.

SECTION V

THE INTERNAL FORCES

This section will analyze the hydrodynamic forces acting on a piece of ice which is separated from a solid surface by a thin film of water and the extent to which they can resist external forces tending to remove the ice. The forces acting in a direction normal to the interface will be considered first.

The normal forces required for removal of the ice are first calculated assuming that all the water under the ice comes from melting of the ice. With no excess water present, the static pressure in the water under the ice differs from the pressure in the surrounding air and is a function of the surface tension of the water and the total curvature of the surface between the water and the air at

the edge of the ice. The difference in the static pressures on the two sides of the air-water surface is given by the following equation:

$$\Delta P = \gamma\left(\frac{1}{R_1} + \frac{1}{R_2}\right), \tag{10}$$

in which ΔP is the pressure difference, γ the surface tension and R_1 and R_2 are the principal radii of curvature of the surface. If the edge of the ice is reasonably straight, the curvature in a plane parallel to the solid surface can be neglected and the total curvature taken in a plane normal to the solid surface.

If an external force acts on the piece of ice, the ice will move to a position of equilibrium in which the force resulting from the pressure difference given in Eq. 10 counterbalances the external force. Since, when the water film is very thin, very slight motion of the ice will produce sizable changes in the curvature of the ice-water interface, the ice will need to move only minutely and will, for all purposes, still be attached to the airfoil surface. For any given water thickness there is, however, an upper limit which the curvature can assume, for the radius of curvature cannot be less than one-half the water thickness. In fact, the minimum radius of curvature can be equal to one-half the thickness only when the contact angle between the fluid and each solid material is zero. The contact angle of water with metal surfaces is greater than zero and a function of the material of the surface, the kind and amount of dirt on the surface, and whether the wetted area is increasing or decreasing. Thus in practical deicing situations the minimum radius of curvature will depend on many uncontrollable factors and be something greater than onehalf the thickness of the water layer. This maximum curvature then determines the maximum ΔP which the water layer can produce and consequently the maximum removal force which the system can resist.

In estimating the maximum pressure difference, ΔP, however, it was assumed in this work that one of the principal radii was one-half of the thickness of the water layer. This assumption leads to low estimates of the pressure in the water under the ice, therefore high estimates of the water thickness required for removal of the ice and high estimates of the time required for removal. This gives an equation

$$(\Delta P)_{max} = \frac{2\gamma}{W} \quad . \tag{11}$$

There remains some question as to the effect of corners where the curvature parallel to the solid surface cannot be neglected. It is obvious that the liquid under the ice cannot extend clear to the sharp corners because this leads to a total surface curvature in the wrong direction to balance the pressure differences. The water film retreats from the corner and rounds it off. The result is that the total curvature becomes the same as at places far from corners, but the wet area is decreased. For large pieces of ice, such as on wings, the area decrease is negligible compared to the total area, but a correction must be made on small models like those used in the present investigation. The force thickness relationship corrected for corners is shown graphically in Fig. 9.

The thickness of water melted can be expressed in terms of the heat flux, the initial temperature of the ice, and the time, as explained previously, and it is therefore possible by using Eq. 11 to establish a relationship between the force required for removal, the heat flux, the initial ice temperature, and the time.

This type of calculation can of course be applied to a specimen of any shape or size on a flat surface and probably equally well to a curved surface with constant radii of curvature. If the surface has a changing curvature, as for instance, the surface of an aircraft wing, then the shape of the water under the ice is a function of the position of the ice on the surface. It therefore becomes essential to consider the possibility and the effects of motion of the ice parallel to the surface. An aircraft wing, for example, is ordinarily a surface with straight-line elements in the span-wise direction and with curvature continuously decreasing with distance aft of the leading edge. If a piece of ice with a water film beneath it slides aft on the surface of the wing, then this water film must become thicker at its center and thinner at the fore and aft edges until some point is reached at which the fore and aft edges of the ice are both in contact with the wing surface. (See the accompanying sketch.) At this point one of several things can happen:

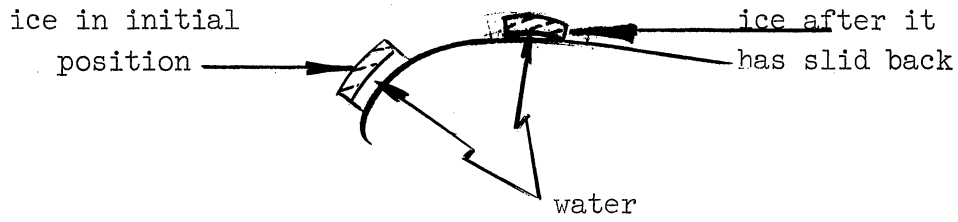

(1) the ice may stop (held in equilibrium by surface tension and pressure forces). (2) The ice may flex and continue to slide aft, bending continuously in such a fashion and amount as to keep a constant water volume beneath it. (3) The ice may break, due to the difference in pressures above and below it, and the fact that it is supported at the fore and aft edges as a beam. (4) The surface tension effect at the sides of the piece of ice may no longer be sufficient to prevent the entrance of air under the ice, therefore, the ice may continue to slide aft while drawing air under it as it slides.

Of course, all these effects may be complicated by continued melting of the ice if the ice is sliding on a warm surface, or by a refreezing of the ice or the water beneath it to the surface of the wing if the ice should slide from a warm to a cold surface of the wing. What actually happens will, of course, be a function of the relationships between the strength and the stiffness of the ice, the surface tension in the water layer, and the relative magnitudes of the forces acting on the ice tangent and normal to the wing surface.

The situation is too complex to be definitely analyzed, but some qualitative conclusions can be drawn. First, tangential motion will not remove the ice by itself. Second, the ice will eventually stop sliding either because it encounters some irregularity on the wing, or because its rear edge moves behind the heated section and becomes frozen fast. If the latter happens, the small frozen part will offer very little resistance to a bending moment caused by removal

forces acting normal to the surface. Observations of deicing tests conducted as part of this investigation indicate that the ice does leave the wing with a motion hinged on its aft end. Figure 10 is a sequence of photographs taken from a high speed motion film and shows the ice shortly after it separates from a model wing.

Finally, it can be seen that if the ice slides aft to a position where it doesn't fit, the average thickness of the water film, which is associated with energy expended, can become greater than the thickness of the front edge, which controls the retaining forces. The heating requirements of the deicing system are thus increased.

Another complication must be considered in more detail. A cyclic-thermal deicer on an airplane wing will normally have a leading-edge parting strip which is kept continuously hot to prevent bridging of the ice over the leading edge of the wing. Water which is melted on this parting strip must run back over the cyclically operated sections of the deicer aft of the parting strip. This runback water may flow under the ice and considerably reduce the time required to remove it.

With no excess water present, the pressure difference between air and the water under the ice is a result of surface tension. With excess water present, the pressure in the water under the ice is a function of the flow velocity and viscosity of the water. Stefan[9] has derived a force-time relationship for the removal of a round solid disk from a flat surface when the disc is immersed in a fluid. His equation is:

$$t = \frac{3}{4} \frac{\mu R^2}{F/A} \left(\frac{1}{W_1^2} - \frac{1}{W_2^2} \right) , \tag{12}$$

in which R is the radius of the disk, μ the viscosity of the liquid, t the time to separate the disc from the base surface, F/A the separation force per unit area, and W_1 and W_2 are the initial and final distance of the disk from the base surface.

In Appendix C a similar relationship is derived for a piece of ice which is infinitely long in one direction, and has a width b in the other. A simplified form of this equation, sufficiently accurate for the values of W encountered in deicing, is

$$t = \frac{1}{4} \frac{\mu}{F/A} \left(\frac{b}{W_1} \right)^2 , \tag{13}$$

where t is the time to remove the ice from initial separation W_1.

The development in Appendix C also yields an equation for the rate of separation

$$\frac{dW}{dt} = \frac{2F}{\mu A b^2} W^3 . \tag{14}$$

The separation resulting from flow and from melting can now be combined for the case when the ice is initially at the melting temperature

$$\frac{dW}{dt} = \frac{2F}{\mu Ab^2} W^3 + \frac{\phi}{\rho L} \quad . \tag{15}$$

This equation can be integrated by separating the variables. Performing the integration and introducing symbols for groups of parameters,

$$\frac{T}{J} = .2647 \left[\frac{1}{2} \ln \frac{(1+B)^2}{(1+B)^2-3B} + \sqrt{3} \tan^{-1} \frac{2B-1}{\sqrt{3}} \right] + .240 \quad , \tag{16}$$

where

$$J = \left(\frac{\mu Ab^2 \rho^2 L^2}{F\phi^2} \right)^{1/3} \tag{17}$$

and

$$B = \frac{W}{k} = \frac{W}{\left(\frac{\mu Ab^2 \phi}{2 F \rho L} \right)^{1/3}} \quad . \tag{18}$$

Equation 16 is plotted in Fig. 11 together with the equation for melting alone which is obtained by dividing Eq. 7 by J and will give

$$t/J = .794 \frac{W}{k} \quad . \tag{19}$$

Examination of Fig. 11 shows that a conservative and simplified design procedure would be to assume that Eq. 19 is correct except that the presence of a sufficient quantity of excess liquid water, for instance as runback from forward deicing heaters, limits the value of t/J to t/J = 1 or t = J.

When the initial temperature of the ice is below its melting point, the equations cannot be solved exactly, but some qualitative conclusions can be made.

Considering the equation developed for melting when heating starts at an initial temperature below melting, i.e.,

$$X = \frac{\phi t_o}{\rho L} S \quad \text{or} \quad W = \frac{\phi t_o}{\rho_w L} S \tag{20}$$

in which

$$S = \frac{2}{\pi} \left[\left(1 + \frac{t}{t_o} \right) \tan^{-1} \left(\frac{t}{t_o} \right)^{1/2} - \left(\frac{t}{t_o} \right) \right]^{1/2} \quad , \tag{21}$$

it can be seen that this can be written

$$Qt = \frac{\rho LW}{\phi} \tag{22}$$

where

$$Q = \frac{S}{t/t_o} \quad . \tag{23}$$

Equation 22 can be divided by J to get

$$Q \frac{t}{J} = .794 \cdot \frac{W}{k} \quad , \tag{24}$$

which aside from the factor Q is the same as Eq. 19.

A more useful form for this equation for design is

$$\frac{St_o}{J} = .794 \frac{W}{k} \quad , \tag{25}$$

since here only S is a function of t, while all the other factors in the equation can be calculated from the design conditions. Thus, S can be calculated and t/t_o can be found from Fig. 12 and multiplied by t_o to get t.

Without excess water, W will be calculated from the surface tension and pressure data. With ample excess water present there is reason to believe that Qt/J and, therefore, St_o/J, will not exceed 1. The basis for this is the following.

The difference between this case and the one in which the ice is initially at its melting point lies only in the loss of some heat to the ice in order to bring its temperature up to the melting point. In Eq. 15 this effect can be accounted for by multiplying ϕ by the factor Q, which is always less than 1. This means that when the initial ice temperature is below the melting point, the effects of heating are relatively less and the effects of flow relatively more than when the initial ice temperature is at the melting point.

Therefore, since the curve of Qt/J vs W/k for melting only and $U_o < 0$ is identical to the curve of t/J vs W/k for $U_o = 0$, it follows that for melting and flow the curve of Qt/J vs W/k for $U_o = 0$ must lie to the right of and below the curve of t/J for $U_o = 0$.

Therefore, the equation,

$$\frac{Qt}{J} = \frac{St_o}{J} = 1.0 \quad , \tag{26}$$

will still give conservative, or high, estimates of the time required for removal of the ice when sufficient excess water is present even though the initial ice temperature is below the melting point.

An interpretation of these results is that when no excess water is available the length of the deicing period is determined by the time required to melt sufficient water to remove the grip of surface tension on the ice. On the other hand, if excess water is present around the edges of the ice, the first part of the deicing period is spent in melting sufficient ice to produce a channel underneath the icecap. Once the channel is formed a relatively short period of time is required for water to flow under the ice and permit it to be removed.

SECTION VI

EXTERNAL FORCES ON THE ICE

The forces acting on the outer surface of ice on an aircraft arise from the air flowing over the surface and the water impinging on it. The aerodynamic forces can be divided into pressure forces acting normal to the surface and viscous drag forces acting parallel to the surface. The forces due to impingement will be approximately tangent to the surface except at the leading edge of an aerofoil, and they may be of the same order of magnitude as the pressure forces.

All these forces tend either to hold the ice in contact with the wing or slide it along the wing surface. To be removed from the surface, the ice must have a component of motion normal to the surface, and this requires the building up of a positive pressure under the ice sufficient to overcome the external forces. If the ice has been deposited on a nonporous surface, the only possible source of this underneath pressure is the external pressure communicated to the water film at the leading edge of the ice. As was shown in Section V, the pressure at the edge of the ice is not communicated with full force to the water film but is diminished by the action of surface tension at the air-water interface. In order to effect ice removal, the pressure at the edge of the ice must be large enough to overcome the effect of surface tension and the pressures acting on the outer surface of the ice cap.

Since an icecap extending around the stagnation point of the wing will have no edge exposed to a high pressure, it will not be subject to any removal forces. This shows why a parting strip is necessary for deicing systems. The parting strip should be wide enough to cover the stagnation point for all angles of attack.

On the basis of these considerations, an ideal method of deicing would be to force hot air under the ice through a porous wing surface. This would achieve the dual purpose of melting the solid bond between the ice and metal and providing directly a high pressure under the ice cap. A minimum of melting would be required, only enough to break the solid bond. Against these advantages must be set the difficulties of controlling the hot air system. A porous wall deicing system offers attractive possibilities and might well be the subject of further study. It is necessary now, however, to return to the calculation of the external forces in a more conventional system.

If the shape of the ice cap is known, the pressure distribution over it can be calculated using the theory of potential flow and analog devices which are applicable to the forward parts of the wing where ice accumulates. If the shape of the ice cap is not known, the pressure distribution can still be obtained with moderate accuracy by taking the pressure distribution over the clean airfoil. This procedure is applicable if the ice cap is not too thick and is a reasonable approximation to the pressure on a piece of ice that forms between heating periods in a cyclic deicing system. It is not a reasonable approximation for obtaining the pressure on ice that deposits over an extended period of time on an unprotected surface.

A special problem arises in calculating the pressure acting at the front edge of the ice cap, and as discussed above this pressure is very important in the removal process. Two possibilities seem reasonable:

1. The pressure at the front edge of the ice is approximately that which would be present at the same point of the clean wing.

2. The pressure at the front of the ice rises to the stagnation pressure of the air stream as a result of the bump caused by the ice deposit.

Theoretical analysis does not offer a simple method of determining which of these hypotheses is correct, but part of the experimental program undertaken in this investigation (described as Series E below) indicates that hypothesis (2) is more nearly correct.

On the forward portion of a wing the pressure decreases with increasing chord. One effect of this is to produce a moment on an ice cap tending to hold the front edge of the ice against the wing and tip the rear edge up. This action is just the contrary of that desired for the removal of a piece of ice floating on a film of water. However, the tangential forces acting on the ice cap cause the ice to start sliding back, and, as explained in lubrication theory, the ice will then tip the other way with the front end up. Thus a small amount of sliding assists the ice removal by increasing the thickness of the water film at the front of the ice and thereby reducing the effect of surface tension, but greater sliding as was shown in Section V carries the ice to a part of the wing with lower curvature and thus impedes the ice removal. It appears then that fortuitous surface irregularities can be a factor in ice removal by affecting the amount of sliding of the ice cap.

To recapitulate, the most important external forces are the aerodynamic pressure forces. Acting on the outside of the ice this pressure tends to hold the ice in place, but the pressure which occurs at the front edge of the ice is communicated to the water layer under the ice and provides a force tending to remove the ice. In the absence of special devices such as porous wing surfaces, ice can be removed only if the pressure at the front edge is greater than the average pressure over the ice cap.

SECTION VII

EXPERIMENTAL PROGRAM

In order to check the theoretical analyses which have been described, an experimental program was undertaken. Six types of experiment were set up, each designed to supplement or verify one or more parts of the theory. A table summarizing the

conditions of each series is given below followed by a detailed description of each series.

Series	Heating rate	U_o	Load	Water thickness	Flow	Deicing
A	slow	<32F	measured	measured	no	no
B	measured	<32F	measured	calculated (force)	no	no
C	measured	<32F	measured	calculated (weight)	no	no
D	measured	<32F	measured	----	yes	no
E	measured	<32F	wind	----	no	no
F	measured	32F	wind	----	?	yes

Test Series A

Series A of the test program was designed to verify the relationship between the thickness of the water film between two solids and the normal force required to separate the two solids. The chief difficulty encountered was the measurement of the thin film of water. Previous investigators have attempted to do this by making a heat balance in which the energy which went into the icecap back of the heater, etc., were subtracted from the total energy input. The difference thus obtained was attributed to heat of fusion which could in turn be interpreted as the thickness of water. Since the heat flow to various parts of the system could not be calculated very accurately, and since the heat of fusion was obtained as a small difference between two larger quantities, this method has not been successful in distinguishing small layers of water. As the problem is studied it becomes evident that accurate measurement of this minute water thickness requires a technique not dependent on heat balances. The present investigators, therefore, developed an ice condenser as an instrument for determining the thickness of thin water layers adjacent to ice. The ice condenser can be operated in a rapid and straightforward manner and gives results which are closely reproducible.

The theory behind the "ice condenser" is quite simple. It is based on the phenomenom that the dielectric coefficient of ice is 3, whereas that of water is 81. Suppose now a condenser is made up with ice as the dielectric instead of an ordinary dielectric such as mica or air (see sketch). As the ice is heated from one side, the capacitance remains constant until melting begins at which time water,

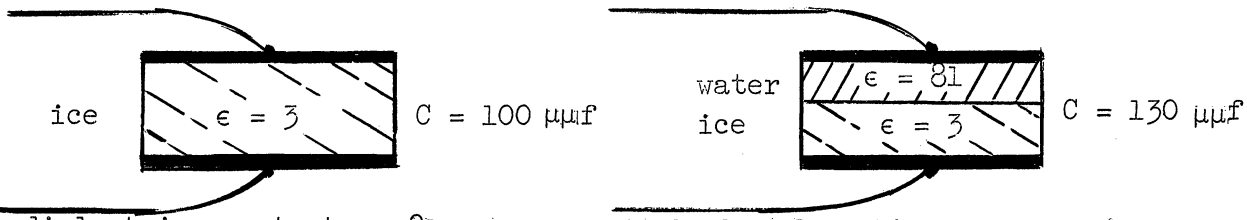

having a dielectric constant of 81, appears at the boundary. As the ice melts to water the total capacitance becomes greater, due to the higher equivalent dielectric constant of the condenser. To measure melting thicknesses, a device need merely be constructed that measures the capacitance of an ice dielectric condenser and detects capacitance changes of 20 to 200 percent accurately. This equipment can be called the "capacitance change detector." Then by making the ice sample to be tested part of a condenser, connecting the ice condenser to the capacitance change detector, and measuring the change in capacity when the ice near the heated surface melts the thickness of water present at any time can be calculated.

A procedure based on the above principles is as follows.

1. Freeze ice between two flat, horizontal, copper disks to have an ice condenser.

2. Connect the ice condenser to a capacitance change detector after determining a, the initial ice thickness, and C_o, the initial capacitance.

3. Load the lower plate with a weight.

4. Uniformly heat the upper copper plate.

5. Melt the ice near the upper plate to a depth Δa and then the ice and lower plate will fall.

6. Monitor the capacitance change during melting and record the total capacitance change ΔC.

7. From ΔC, C_o, and a, compute Δa, the melting depth.

8. Repeat with a series of weights to obtain the relationship of force to Δa.

A schematic representation of the equipment is illustrated. The equipment required and the procedure are discussed in detail in Appendix D.

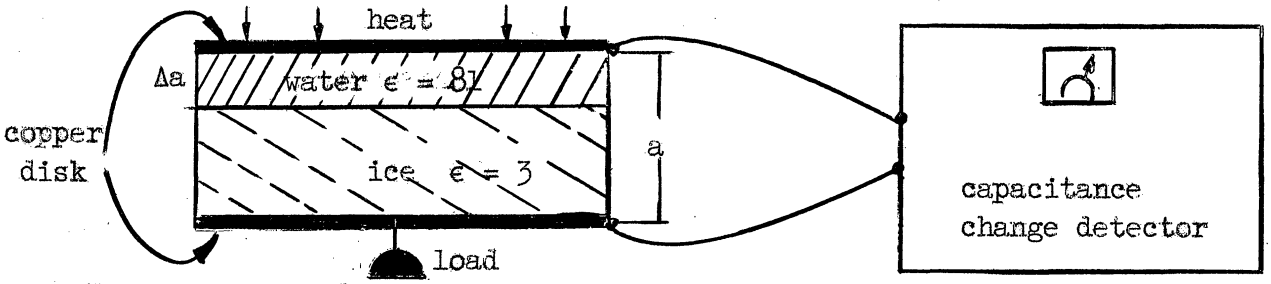

It has been predicted by surface tension considerations that the relationship between water thickness Δa and pressure P should be one of approximately inverse proportionality or

$$\Delta a = 2\gamma/P \quad ,$$

where γ is the surface tension constant (75.5 dynes/cm). This relationship is verified by the ice condenser experiment as indicated in Fig. 13. The heavy line is the predicted curve while the crosses are the average values of Δa obtained at each particular normal pressure.

Test Series B

Series B tests were designed to verify the relationship between initial temperature, heating rate, and removal force. Pieces of ice approximately 2" x 2" x .25" were frozen on an electrical heating element and were removed by heating at a known rate, starting at a known initial temperature ($<0°C$), and

under a known normal force. The time required for removal was accurately measured. The setup for this test is shown in Fig. 14.

The heater element consisted of a piece of 2" x .002" nichrome ribbon 2.5 inches long with .25" x .03" copper strips soldered to its ends to make electrical connections. This made a 2" x 2" heating element which was cemented to a 6" x 2" x .5" piece of varnished balsa wood in order to have a rigid backing which would take up as little heat energy as possible. The force was applied by weights through a string and lever system as shown in the photograph.

Not shown in the photograph are the autotransformer controlled a-c power supply, the electric clock timer, the microswitch used for automatic power and timer cutoff, and the lead weights used to hold down the balsa wood heater backing.

The automatic cutoff microswitch was mounted at the top of the framework shown in the photograph and was actuated by a less than one-quarter inch movement of the lever. The microswitch in turn actuated a relay which cut off both the electric timer and the power to the heater. In early tests the timer was only accurate to one-half second, but in later tests a different timer was used whose accuracy was limited only by the actuating system and was probably good to .05 second.

The test procedure went as follows.

1. The 1.75" square x .25" thick ice blocks were made in a mold and wire loops fastened to the top by melting them into the ice and then refreezing.

2. These ice blocks were removed from their molds by melting, mounted on the chilled heaters with the aid of about .5 cc of additional ice water and frozen into place.

3. The ice and heater were placed in the test framework with a thermometer lying adjacent to the ice, all connections were made and the whole setup allowed to come to an equilibrium temperature; a matter of twenty to thirty minutes.

4. With the load and heater voltage adjusted the timer and heater power were turned on with a single switch, the heater voltage and current were read during the test, and the timer and heater power were turned off automatically by the microswitch.

The above procedure yields the following data:

the normal force for separation,
the initial temperatue of the ice, U_o,
the heater current I,
the heater voltage E, and
the time required for the ice to be separated from the heater, $(t + t_o)$.

From this data the following can be found.

$$\phi = \frac{EI}{4.185\ (19.75)} = \text{the heating rate}$$

$$t_o = \frac{\pi}{4}\frac{Kc\rho U_o^2}{\phi^2} = \text{time for melting to start}$$

$$\frac{t}{t_o} = \frac{t + t_o}{t_o} - 1 = \text{dimensionless time}$$

W = water layer thickness required for separation based on calculations of the force-surface tension-area relations for the ice sample. (Fig. 9).

For comparison with theoretical results the quantity $\rho LW/\phi t_o$ is plotted against t/t_o. In the theory the results should be approximately

$$\frac{\rho LW}{\phi t_o} = \frac{2}{\pi}\left[\left(1 + \frac{t}{t_o}\right)\ \tan^{-1}\ (t/t_o)^{1/2} - (t/t_o)^{1/2}\right]$$

The experimental results are plotted as open circles in Fig. 8. The force-thickness relation used should lead to high values for the thickness and the locations of the circles seem to bear this out.

This series of tests indicate that the theoretical results are substantially correct and will be slightly conservative if used as the basis for design.

Test Series C

This series of tests is in fact a part of the B series in which one extra set of measurements was made. The extra measurements consisted of weighing the ice plus heater and heater base before each test. Then after the test the heater and heater base and the ice were wiped dry with a sponge and again weighed.

The object of this procedure was to obtain another estimate of the amount of water melted. It is believed that this process should usually lead to a low estimate of the amount of water melted, chiefly because of the refreezing of melted water on the ice sample after its release from the heater.

The value of W so estimated was used to compute a new value of $\rho LW/\phi t_o$ and these values are plotted on Fig. 8 as the filled-in circles. The locations of these circles tend to substantiate the belief that the estimate of W is low. Conversely, if the judgments that W is estimated too low in test series C and too high in test series B is accepted, then these two series of tests show the theoretical curve to be substantially correct.

Test Series D

This series of tests was designed to verify Eq. 26. Test series D was like series B except the heater was mounted on a larger balsa wood base and was surrounded by a piece of one-quarter inch plexiglass to provide a reservoir of

of excess water (see Fig. 15). The excess water, slightly above freezing temperature, was added just before the heater power was turned on to simulate the pressure of runback water in an airplane deicing system.

In calculating results from these tests the value $W/k = 10$ was arbitrarily chosen as corresponding to the release of the ice. A different choice would produce a negligible change in the results because of the rapid increase of W with t.

The results of this series of tests are plotted in Fig. 11 and show that the analysis leading to Eq. 26 is substantially correct.

Test Series E

In the series E tests it was assumed that series A, B, and C had demonstrated the validity of the analysis and that a test in a wind tunnel could be used to get some estimate of the forces available for the removal of the ice, provided of course that the first motion of the ice was predominately normal to the wing surface. In particular, the tests were designed to decide whether hypothesis 1 or 2 of Section VI gave a reasonable estimate of the forces.

The tests were run in a 4" x 6" single-pass wind tunnel operating in a refrigerated room at about 100 fps test section velocity. The heater in these tests was a 3/4" wide by 5" long strip of silver paint (manufactured by a General Cement Company) sprayed onto a hollow plexiglas airfoil 1.2" thick and with a chord of 7.5". (Approximately NACA 65_2-016 profile, see Fig. 16).

Pieces of ice 3.06" x .56" x, roughly, 1/8" were frozen in place on the heater strip with the airfoil in the wind tunnel and the fan on to hasten freezing. When the ice was frozen, the mold was removed, the sharp corners removed from the ice with a soldering iron, and additional time allowed for the ice to reach an equilibrium temperature. The test was then run very much as were the series B tests, except that the removing force was aerodynamic and shutting off, as well as the starting of the heating and timing, was manually controlled.

The data taken included:

the initial temperature,
the voltage across the heater including the leads,
the current to the heater, and
the time to remove the ice.

There was, of course, some voltage drop in the leads, but space limitations prevented measuring the voltage drop across the heater alone. The loss in the leads was less than 1 percent of the total voltage drop.

In analyzing the data from this set of experiments the pressure on top of the ice was assumed to equal that at the chordwise station corresponding to the midpoint of the ice on an NACA 65_2-015 airfoil at zero angle of attack as given by NACA Report 824, Summary of Airfoil Data. The pressure on the front surface of

the water layer, i.e., at the leading edge of the ice, was assumed to be equal to the stagnation pressure, i.e., hypothesis 2 was employed. The difference of these two pressures was taken as the F/A which had to overcome the negative pressure in the water layer due to surface tension effects before the ice would come off the airfoil. With these assumed pressures J, k and W could be calculated.

The dimensionless time, $St_o/J = Qt/J$ and the dimensionless thickness W/k, were then calculated and plotted in Fig. 11. The points correspond reasonably well to the theoretical curve, but indicate that the pressure difference used for the calculations should be reduced by about 25 percent. Points obtained with a 30 percent lower pressure difference are also plotted in Fig. 11 and show good agreement. The 25 percent difference is not surprising when it is remembered that the airfoil shape has been altered by the ice accretion and that the angle of attack was not precisely set at 0. In contrast, the values of ΔP that would be obtained by using hypothesis 1 are about 2 percent of the values required to give agreement with the theoretical curve. Thus, this series of tests definitely supports hypothesis 2, that the pressure at the leading edge of the ice is the stagnation pressure.

Test Series F

This series of tests was made in the University of Michigan icing wind tunnel which has since been destroyed by fire.

The wing model consisted of a 6" span, 7.5" chord NACA 65_2-016 airfoil section made of balsa wood and overlaid with copper foil on its forward portion. The development of this model is described in Appendix E and its dimensions are given in Fig. 19. The heaters used were the forward ones on each side of the airfoil between approximately the 1.7 percent chord point and the 11.7 percent chord point. The tests were run at several heating rates and several tunnel air velocities.

The test procedure consisted of turning on the heaters for a predetermined time, then turning them off and recording whether or not the ice had come off. If the ice had not come off some time was allowed for the system to cool to equilibrium temperature, then another trial was made using a longer heating time. The longest time not causing shedding and the time which caused shedding were then recorded.

The equilibrium temperature of the ice was between 31.5 and 32°F with the heaters off even though the tunnel temperature was 28°F. This was due to aerodynamic heating, plus heat given up by the supercooled water as it froze. The results are plotted directly in Figs. 17 and 18 and in the nondimensional forms developed for test series B, C, and D in Fig. 20.

The data do not match the theoretical curve nearly as well as the other series of tests. This can be partially attributed to poor control of time intervals and angle of attack of the model as well as some uncertainty as to the actual profile of the model.

Comparison of Fig. 20 and Fig. 11 indicates pretty clearly, however, that the ice on the model is not surrounded by a great deal of excess water and,

thereofre, that surface tension is a controlling factor in the amount of water which must be melted to get shedding of the ice. The difference between the stagnation pressure and the local pressure on a clean wing at the leading edge of the ice is not great enough in these tests to make a clear cut decision as to which is the correct one to use in computing the forces on the ice. Use of the clean wing local pressure will give more conservative results and would be about right for some of these lists, but could be way off for the aft heaters.

Conclusions from Experiments

Taken as a whole the experiments show that the theoretical treatment is substantially correct and may be relied on to predict the influence of various parameters on the performance of deicing equipment. The numerical values obtained from the theory were of the right order of magnitude and usually within 20 or 30 percent of the values obtained experimentally. There were two questions which the theory could not resolve and for which alternative procedures were offered. The experiments gave evidence that runback water did not play an important role in ice removal and that the pressure on the water at the forward edge of the ice was the stagnation pressure. However, the alternative should not be ruled out finally until tested further on larger models.

APPENDIX A

EQUATIONS FOR ANALOG COMPUTATION

The difference equations governing the flow of energy in the network of Fig. 3 have the form

$$\text{(A1)} \qquad \sum_{y} G_{y-n} (U_y - U_n) = C \frac{dU_n}{dt} \quad ,$$

where
- n = the cell at which the heat balance is being made
- y = an adjacent cell
- G_{y-n} = thermal conductance between cell pairs
- $C = V\rho C_\rho$ = the thermal capacitance of the cell Btu/°F
- $\frac{dU_n}{dt}$ = rate of change of temperature of the nth cell = °F/hr
- K = thermal conductivity = energy/time-distance-temperature
- A = area of heat flow = ft^2
- V = volume = ft^3
- a = length of heat flow = ft
- ρ = density = lb/ft^3

In addition, Cell 7 receives energy from an external source. The energy balance then is given by

$$\text{(A2)} \qquad \text{Power in} + \sum_{y} \frac{G_{y-7}}{M} (U_y - U_7) = C \frac{dU_7}{dt} \quad .$$

The values of the physical properties of the system are given below.

PHYSICAL PROPERTIES OF BOOT MATERIALS AND ICECAP

Material	Density lb/cu ft	Specific Heat Btu/lb-F	Thermal Conductivity Btu/hr-ft-F
Aluminum	160	00.178	117
Neoprene	75	0.40	0.073
Nylon	66	0.55	0.145
Ice	57	0.46	1.28
Nichrome	515	0.193	----

When the materials of adjacent cells are different, the thermal conductance G_{y-n} is obtained as the reciprocal of the thermal resistance between the n and y cells. This in turn is calculated by adding the thermal resistance of one-half the n cell to one-half the resistance of the y cell. An example calculation for Cell No. 1 will illustrate the method.

For Cell 1 the dimension of the cell normal to page (in Fig. 3) is taken as one foot.

$$G_{2,1} = \frac{KA}{a} = \frac{(1.28)(0.067)(12)}{(0.00975)(12)} = 9.02 \text{ Btu/hr-F}$$

$$G_{4,1} = \frac{1}{\frac{1}{2}\frac{a}{kA)_1} + \frac{1}{2}\frac{a}{kA)_4}} = \frac{1}{\frac{(0.033)(12)}{(1.28)(0.0065)(12)} + \frac{(0.011)(12)}{(0.073)(0.0065)(12)}} = 0.0368 \text{ Btu/hr-F}$$

$$C_1 = V\rho c_p = \frac{(0.067)(0.0065)}{(12)(2)} (57)(0.46) = 7.92 \times 10^{-5} \text{ Btu/F}$$

Then Eq. 1 becomes

$$11.390 + 10^4 U_2 + 0.0463 \times 10^4 U_4 - 11.437 \times 10^4 U_1 = \frac{dU_1}{dt} .$$

Making the substitution $T = 10^4 t$ gives

$$11.390\ U_2 + 0.0463\ U_4 - 11.437\ U_1 = \frac{dU_1}{dT} .$$

The complete set of equations for the thirteen cells is given in the following table.

These equations were set up for simultaneous solution on a differential analyzer and voltages corresponding to temperatures were plotted against time to give the curves of Fig. 4.

DIFFERENTIAL EQUATIONS FOR HEAT CONDUCTION THROUGH RUBBER DEICER BOOT

$$\frac{dU_1}{dT} = 11.390\ U_2 + 0.0463\ U_4 - 11.461\ U_1$$

$$\frac{dU_2}{dT} = -5.919\ U_1 - 4.502\ U_3 - 0.0463\ U_5 + 10.514\ U_2$$

$$\frac{dU_3}{dT} = 4.502\ U_2 + 0.0463\ U_6 - 4.595\ U_3 +$$

$$\frac{dU_4}{dT} = -0.1235\ U_1 - 0.5676\ U_5 - 0.1447\ U_7 + 0.8359\ U_4$$

$$\frac{dU_5}{dT} = 0.2951\ U_4 + 0.1234\ U_2 + 0.2242\ U_6 + 0.1115\ U_8 - 0.7543\ U_5$$

$$\frac{dU_6}{dT} = -0.2243\ U_5 - 0.1234\ U_3 - 0.1115\ U_9 + 0.4592\ U_6$$

$$\frac{dU_7}{dT} = 0.0742\ U_4 + 0.5180\ U_8 + 0.0204\ U_{10} - 0.6131\ U_7 + q/0.5817$$

$$\frac{dU_8}{dT} = 0.7353\ U_7 - 0.1558\ U_5 + 0.3676\ U_9 - 0.0515\ U_{11} + 1.310\ U_8$$

$$\frac{dU_9}{dT} = 0.3676\ U_8 + 0.1558\ U_6 + 0.0515\ U_{12} - 0.5749\ U_9$$

$$\frac{dU_{10}}{dT} = -0.0110\ U_7 - 0.5665\ U_{11} - 0.0110\ U_{13} + 0.5885\ U_{10}$$

$$\frac{dU_{11}}{dT} = 0.2948\ U_{10} + 0.0101\ U_8 + 0.2241\ U_{12} + 0.0109\ U_{13} - 0.5399\ U_{11}$$

$$\frac{dU_{12}}{dT} = -0.2241\ U_{11} - 0.0101\ U_9 - 0.0109\ U_{13} + 0.2451\ U_{12}$$

$$\frac{dU_{13}}{dT} = .0015\ U_{10} + 0.0026\ U_{11} + 0.0029\ U_{12} - 0.0073\ U_{13}$$

APPENDIX B

THE PROBLEM OF MELTING ICE AT CONSTANT HEAT FLUX

Consider a one-dimensional semi-infinite slab of ice at a constant initial temperature, $-U_o$, corresponding to that of the air and with a constant heat flux ϕ applied at the finite boundary. After a time t_o the boundary reaches the melting point which has temperature 0, and an ice-water interface begins to move through the material. The problem to be considered is the determination of the position of this interface as a function of time and the parameters ϕ and U_o.

Problems of this type have been treated by Stefan and others, but the boundary conditions in the case considered here are such that it appears unlikely than an exact solution can be found; however, it is possible to "linearize" the temperature equations in a manner which permits a good approximation for the ranges of the variables which are important for aircraft deicing. It is assumed that the loss of heat energy to the water is negligible compared to the total amount introduced; that is, the heat flux ϕ goes into two places, to melt the ice and to raise the temperature of the ice.

The determination of the temperature distribution in the ice at the time melting begins is a linear problem and its solution by use of the Laplace transformation is well known. If the time t is measured from the instant melting begins and distance x from the finite boundary, i.e., the place at which the heat is applied, the boundary value problem is as follows:

$$\text{(B1)} \qquad \frac{\partial U}{\partial t} = \alpha \frac{\partial^2 U}{\partial x^2} \qquad X(t) \leq x < \infty,\ t > 0 \ ,$$

$$\text{(B2)} \qquad U(x,0) = \left[-U_o - \frac{\phi}{k} \sqrt{4\alpha t_o}\ \text{ierfc}\left(\frac{x}{\sqrt{4\alpha t_o}} \right) \right] \ ,$$

$$\text{(B3)} \qquad U(X(t),t) = 0 \ ,$$

$$\text{(B4)} \qquad \lim_{x \longrightarrow \infty} U(x,t) = -U_o \ ,$$

$$\text{(B5)} \qquad \phi = \rho L \frac{dX}{dt} + K \frac{\partial U}{\partial x}(X(t),t) \ ,$$

where $U(x,t)$ is the temperature distribution in the ice,

The α, K, L and ρ are the diffusivity, conductivity, heat of fusion, and density respectively of ice,

t_o is the time between power on and the start of melting, and ierfc is the integral of the complementary error function.

The position of the ice-water interface is X(t) and consequently gives the thickness of ice melted as a function of time. By making a transformation of the space coordinate z = x-X(t), the position of a point in the ice is related to that of the moving interface and the problem takes the form:

$$\alpha \frac{\partial^2 U}{\partial z^2} = \frac{\partial U}{\partial t} - \frac{\partial U}{\partial z}\frac{dX}{dt} \tag{B6a}$$

$$U(z,0) = -U_o + \frac{\phi}{K}\sqrt{4\alpha t_o}\ \text{ierfc}\left(\frac{-z}{\sqrt{4\alpha t_o}}\right) = F(z) \tag{B7}$$

$$U(0,t) = 0 \tag{B8}$$

$$\lim_{z \longrightarrow \infty} U(z,t) = -U_o \tag{B9}$$

$$\phi = \rho L \frac{dX}{dt} + K \frac{\partial U}{\partial z}(0,t) \tag{B10}$$

$$X(0) = 0 \tag{B11}$$

An examination of Eq. B6a shows the nonlinear property of the system which makes it invulnerable to the various methods of attack known in partial differential equations. At this point a second major assumption is introduced which will "linearize" the above system, and hence, give a suitable approximation to the solution for X(t).

Because of physical considerations, only the values of X(t) for a small range of t, say $0 < t < 20$ seconds, will be necessary here. Thus, if the term $-\dot{X}(\partial U/\partial z)$ is small compared to the other quantities in Eq. B6a, the solution obtained by dropping this term will be close to the exact one.* If this is done, the rest of the problem, i.e., satisfying the boundary conditions and calculating X(t), goes through quite readily. Using the results obtained by this method, the quantity $-\dot{X}(\partial U/\partial z)$ can be evaluated and in some degree the plausibility of its neglect determined.

The solution to the linearized boundary value problem can be obtained by use of the Laplace transformation as is stated in Reference 2. The problem is to solve

$$\alpha U_{zz} = U_t \tag{B6b}$$

$$U(z,0) = F(z) \tag{B7}$$

$$U(0,t) = 0 \tag{B8}$$

$$\lim_{z \longrightarrow \infty} U(z,t) = U_o \tag{B9}$$

Let

$$U(z,s) = \text{Laplacian}\ \left\{U(z,t)\right\}$$

* Dropping the term is equivalent to setting Landau's m = 0.

Then

$$sU(z,s) - F(z) = \alpha U_{zz}(z,s)$$

$$U_{zz} - \frac{s}{\alpha} U = -\frac{F}{\alpha}$$

$$U(0,s) = 0$$

$$\lim_{z \to \infty} U(z,s) = -\frac{U_o}{s}$$

$$U(z,s) = C_1 e^{\sqrt{\frac{s}{\alpha}} z} + C_2 e^{-\sqrt{\frac{s}{\alpha}} z} + U^*.$$

The U* is obtained by the method of variation of parameters

$$U(z,s) = c_1 e^{\sqrt{\frac{s}{\alpha}} z} + c_2 e^{-\sqrt{\frac{s}{\alpha}} z} - \frac{1}{2}\sqrt{\frac{\alpha}{s}} \left[\int_x^\infty e^{\sqrt{\frac{s}{\alpha}}(z-\lambda)} \frac{F(\lambda)}{\alpha} d\lambda + \int_0^x e^{-\sqrt{\frac{s}{\alpha}}(z-\lambda)} \frac{F(\lambda)}{\alpha} d\lambda \right]$$

After lengthy, but straightforward calculation, the expression for U(z,s) becomes

$$U(z,s) = -\frac{1}{2}\sqrt{\frac{\alpha}{s}} \int_0^\infty \left\{ e^{-\sqrt{\frac{s}{\alpha}}(x-\lambda)} - e^{-\sqrt{\frac{s}{\alpha}}(x+\lambda)} \right\} \frac{F(\lambda)}{\alpha} d\lambda .$$

From a table of inverse transforms

$$\text{Inverse Laplacian} \left\{ \frac{e^{-k\sqrt{s}}}{\sqrt{s}} \right\} = \frac{1}{\sqrt{\pi t}} e^{-\frac{K^2}{4t}} \qquad (K \geq 0) .$$

Applying this formally above

$$U(z,t) = -\frac{\sqrt{\alpha}}{2\alpha} \int_0^\infty \left\{ \frac{1}{\sqrt{\pi t}} e^{-\frac{(x-\lambda)^2}{4\alpha t}} - \frac{1}{\sqrt{\pi t}} e^{-\frac{(x+\lambda)^2}{4\alpha t}} \right\} F(\lambda) d\lambda$$

(B12)
$$U(z,t) = \frac{1}{\sqrt{4\pi\alpha t}} \int_0^\infty \left\{ e^{-\frac{(x+\lambda)^2}{4\alpha t}} - e^{-\frac{(x-\lambda)^2}{4\alpha t}} \right\} F(\lambda) d\lambda.$$

This result is easily verified by differentiation to be a solution of the equation. Then U(0,t) = 0 is obvious, but the other boundary conditions are more easily seen to hold by a change of variable, e.g., $x + \lambda = \xi$.

Equation B12 can be differentiated with respect to z; z is set equal to zero and expressions B10 and B11 are used to find X(t).

*Dropping the term is equivalent to setting Landau's m = 0.

$$\frac{\partial U}{\partial z}(z,t) = \frac{1}{\sqrt{4\pi\alpha t}} \int_0^\infty F(\xi)\left\{ \frac{2(\xi-z)}{4\alpha t} e^{-\frac{(\xi-z)^2}{4\alpha t}} + 2\frac{(\xi-z)}{4\alpha t} e^{-\frac{(\xi+z)^2}{4\alpha t}} \right\} d\xi$$

$$\frac{\partial U}{\partial z}(0,t) = \frac{-1}{\sqrt{\pi\alpha t}} \int_0^\infty F(\xi) \frac{-\xi}{2\alpha t} e^{-\frac{-\xi^2}{4\alpha t}} d\xi \quad .$$

Integrating by parts

(B13) $$\frac{\partial U}{\partial z}(0,t) = \frac{-1}{\sqrt{\pi\alpha t}} \left\{ F(\xi) e^{-\frac{\xi^2}{4\alpha t}} \Big|_0^\infty - \int_0^\infty F^1(\xi) e^{-\frac{\xi^2}{4\alpha t}} d\xi \right\}$$

$$= \frac{1}{\sqrt{\pi\alpha t}} \int_0^\infty F^1(\xi) e^{-\frac{\xi^2}{4\alpha t}} d\xi \quad .$$

From Eq. B7,

$$F^1(\xi) = \frac{\phi}{K}\left\{ 1 - \frac{2}{\sqrt{\pi}} \int_0^{\frac{\xi}{\sqrt{4\alpha t_o}}} e^{-\lambda^2} d\lambda \right\} \quad .$$

Changing variables and collecting terms

$$\frac{\partial U}{\partial z}(0,t) = \frac{\phi}{K}\left\{ 1 - \frac{4}{\pi} \int_0^\infty e^{-\tau^2} \int_0^{\tau\sqrt{\frac{t}{t_o}}} e^{-\lambda^2} d\lambda d\tau \right\} \quad .$$

Expression B13 can be simplified as follows:

Define $$g(y) = \int_0^\infty e^{-t^2} f(y,t)dt \quad \text{and} \quad f(y,t) = \int_0^{ty} e^{-\lambda^2} d\lambda$$

where $$y = \sqrt{\frac{t}{t_o}}$$

$$\frac{\partial f}{\partial y} = te^{-t^2y^2} \quad \text{and} \quad \frac{\partial g}{\partial y} = \int_0^\infty te^{-t^2} e^{-t^2y^2} dt$$

$$\frac{\partial g}{\partial y} = -\frac{1}{2} \int_0^\infty -2te^{-t^2(1+y^2)} dt$$

$$\frac{\partial g}{\partial y} = -\frac{1}{2} \frac{e^{-t^2(1+y^2)}}{(1+y^2)} \Big|_0^\infty = \frac{1}{2(1+y^2)}$$

Integrating: $g(y) = \frac{1}{2}\tan^{-1}y+c$, but since it is easily seen that $g(0) = 0$, $c = 0$.

The simplified expression for B13 is

$$\text{(B14)} \qquad \frac{\partial U}{\partial z}(0,t) = \frac{\phi}{K}\left\{1 - \frac{2}{\pi}\tan^{-1}(t/t_o)^{1/2}\right\}$$

From Eq. B10

$$\rho L \frac{dX(t)}{dt} = -K\frac{\partial U}{\partial z}(0,t) + \phi \quad .$$

Substituting Eq. B14

$$\rho L \frac{dX}{dt} = \phi\left(1 - \frac{2}{\pi}\tan^{-1}(t/t_o)^{1/2}\right) + \phi$$

$$\rho L \frac{dX}{dt} = \phi\frac{2}{\pi}\tan^{-1}(t/t_o)^{1/2}$$

$$\frac{dX}{dt} = \frac{2\phi}{\pi\rho L}\int \tan^{-1}(t/t_o)^{1/2}dt + c$$

$$x(t) = \frac{2\phi}{\pi\rho L}\left[(t/t_o)\tan^{-1}(t/t_o)^{1/2} - (t/t_o)^{1/2}\right] + c.$$

e last step can be verified easily be differentiation.)

Since from Eq. 11 $X(0) = 0$, $c = 0$, and the final result for $X(t)$ is

$$\text{(B15a)} \qquad X(t) = \frac{2\phi}{\pi\rho L}\left\{(t+t_o)\tan^{-1}(t/t_o)^{1/2} - (t/t_o)^{1/2}\right\} \quad .$$

This is the result sought. So $X(t)$ depends on the ice properties ρ and L and the parameters ϕ and t_o. Incidentally, t_o can be eaily calculated and is given in Reference 2 as

$$\text{(B15b)} \qquad t_o = \frac{U_o^2K^2\pi}{\alpha\phi^2 4} \quad .$$

It is now possible to calculate the neglected term $-\dot{X}(\partial U/\partial z)$ and compare it with the other terms in Eq. B6a. Since the remaining terms are set equal for all values of z and t, either one is suitable for the following definition

$$\text{(B16)} \qquad R(z,t) = \frac{-\dot{X}\frac{\partial U}{\partial z}}{\frac{\partial^2 U}{\partial z^2}} \quad .$$

Of particular interest is

$$(B17) \qquad R(X(t),t) = \frac{\dot{X}\left\{ \operatorname{erfc} \frac{X(t)}{\sqrt{4\alpha(t+t_o)}} - \frac{2}{\pi} I(t) \right\}}{\frac{2\alpha}{\sqrt{\pi}\sqrt{4\alpha(t+t_o)}} \left\{ e^{-\frac{X^2}{4\alpha(t+t_o)}} \operatorname{erfc} \frac{X\sqrt{t}}{\sqrt{t_o}\sqrt{4\alpha(t+t_o)}} \right\}}$$

where

$$I(t) = \int_0^{\sqrt{\frac{t}{t_o}}} \frac{e^{-\frac{X^2(1+\lambda^2)}{4\alpha(t+t_o)}}}{(t+\lambda^2)} \, d\lambda$$

(The above results were obtained from Eqs. B12, B15a, and B16 by tedious integrations.)

Equation B17 now gives R as a function of t alone. Calculations showed that $0 < R(t) < .10$ for $t < 20$ seconds. It is important to note here that this bound on $R(t)$ does not guarantee a definite limit on the error in $X(t)$, but only gives a strong indication that it is small. A possible way of improving the result for X might be to approximate the term $-\dot{X}(\partial U/\partial z)$ by the expression B17 and to use a successive approximation attack. However, there are other reasons to believe that this will not be necessary for the range of quantities of interest.

After the work of this paper had been substantially completed, an article by Landau[4] was discovered which contained these results as part of a larger undertaking. Landau considered the problem as stated in Eqs. B6 through B11 but without dropping the term $-\dot{X}(\partial U/\partial z)$. Instead he defined the problem in the following way using the parameter $m = \sqrt{\pi c(-U_o)/2L}$ where c is the specific heat of ice:

$$(B18) \qquad \frac{\partial U}{\partial t} = \frac{\partial^2 U}{\partial z^2} + m\mu(t) \frac{\partial U}{\partial z} \qquad z > 0, \; t > 0$$

$$(B19) \qquad U(z,0) = \operatorname{ierfc}\left(\frac{z}{2}\right)$$

$$(B20) \qquad \lim_{z \to \infty} U(z,t) = 0$$

$$(B21) \qquad \mu(t) = 1 + 2 \frac{\partial U}{\partial z}(0,t)$$

$$(B22) \qquad U(0,t) = \frac{1}{\sqrt{\pi}} \qquad t \quad 0$$

Equations B18 through B12 look somewhat different from B6a through B11, because the variables have been made dimensionless and $\mu(t)$ corresponds to the rate of change of the interface position. Using the facilities of high-speed computers,

Landau was able to obtain solutions for several values of the parameter m. In particular, the solution for m = 0 (a physically nonrealizable case) corresponds exactly to the approximation obtained here. Actually in deicing problems m will seldom exceed .2. Lanau's results show that the solutions for m = 0 and m = .2 are close enough for the ranges of the quantities considered here and B15a will be within 10 percent of the solution for the exact value of m.

It is important to note here that the quantity X(t) is the thickness of ice melted, not the thickness of the resulting water layer. This difference is important in computing the forces required to remove the ice from the surface.

APPENDIX C

RELATIONSHIP OF ICE REMOVAL FORCES TO WATER FLOW UNDER THE ICE

If two parallel, flat surfaces submerged in a viscous fluid are being separated by forces normal to the surfaces, the relationship between the forces, the time since their application, and the distance between the plates is a function of the size and shape of the plates and the viscosity of the fluid provided the motion is slow enough so that inertia forces can be neglected. Also, if vertical motions are small, gravity forces can be neglected as well.

In deicing problems the conditions for neglecting gravity forces are likely to be met and though inertia forces may not themselves be negligible, the increments of time during which they are important will be extremely short so that their effect on the time and energy required for ice removal will be negligible. It also seems likely that surface curvature will have little effect so long as the radius of curvature is large compared to the dimensions of the piece of ice under consideration.

Stefan[9] gave a solution with experimental verification for this type of problem in 1874. He dealt with a disk being separated from a much larger parallel surface while submerged in various fluids, one of which was water. His solution is

$$\frac{F}{A} = \frac{3}{4}\frac{\mu R^2}{t}\left(\frac{1}{W_1^2} - \frac{1}{W_2^2}\right) \quad , \tag{C1}$$

where
- R = radius of disk
- μ = viscosity of fluid,
- t = time,
- W_1 = initial separation distance,
- W_2 = final distance,
- F = normal force on disk, and
- A = area of disk.

Considering other uncertainties involved, this should be a sufficiently good approximation for a square specimen and other shapes with roughly similar dimensions in all directions. Since some pieces of ice are likely to be long and narrow, however, another expression has been derived based on similar assumptions, except that the piece of ice was assumed to be infinitely long in one direction and of width b in the other. The derivation follows.

The problem is simplified somewhat by making it symmetrical, that is, two similar plates are used which are of infinite length, of width 2a, and are separated by a distance 2h. The axes are chosen as shown in the accompanying sketch with velocities in the fluid of u and v in the x and y directions, respectively.

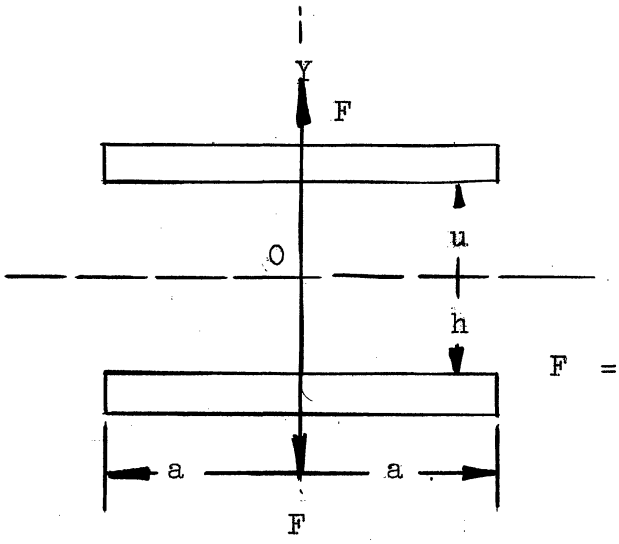

F = force per unit length in Z direction in y direction

With "body" forces and inertia forces neglected, Navier Stokes equations for the fluid motion in two dimensions reduce to

$$\left\{ \begin{array}{l} \dfrac{\partial P}{\partial x} = \mu\left(\dfrac{\partial^2 u}{\partial x^2} + \dfrac{\partial^2 u}{\partial y^2}\right) \\ \dfrac{\partial P}{\partial y} = \mu\left(\dfrac{\partial^2 v}{\partial x^2} + \dfrac{\partial^2 v}{\partial y^2}\right) \end{array} \right\} . \tag{C2}$$

The boundary conditions are

$$\left\{ \begin{array}{l} u = 0 \quad \text{for} \quad y = \pm h \\ u = 0 \quad \text{for} \quad x = 0 \\ v \text{ is not a function of X for } y = \pm h \end{array} \right\} . \tag{C3}$$

It can be seen that Eqs. C2 and C3 are completely satisfied by the following equation.

$$\left\{ \begin{array}{l} P = C(x^2 + y^2) \\ u = \dfrac{Cx}{\mu}(y^2 - h^2) \\ v = \dfrac{C}{\mu}\left(\dfrac{y^3}{3} - h^2 - y\right) \end{array} \right\} . \tag{C4}$$

The value of F can now be found by integration of P over the surface, y = h, thus

$$\left\{ \begin{array}{l} F = -2\displaystyle\int_0^a C(x^2 + h^2)\, dx \\ \quad = -2\left(\dfrac{Ca^3}{3} + Ch^2 a\right) \end{array} \right\} , \tag{C5}$$

and the average force per unit area is

$$F/A = -C\left(\frac{a^2}{3} + h^2\right) ,$$

from which

$$C = -\frac{F/A}{\frac{a^2}{3} + h^2} .$$

The notation can now be changed back to its original form by substituting

(C8)
$$\left.\begin{aligned} a &= \frac{b}{2} \\ h &= \frac{W}{2} \\ v &= \frac{1}{2}\frac{dW}{dt} \quad \text{for} \quad y = h \end{aligned}\right\}$$

to give

(C9)
$$\frac{dW}{dt} = \frac{2\frac{F}{A}W^3}{\mu(b^2 + 3W^2)} .$$

In this equation the variables are separable and integration is easy.

$$\int_{W_1}^{W_2} \frac{b^2 + 3W^2}{W^3}\, dW = \frac{2}{\mu}\left(\frac{F}{A}\right)\int_0^t dt$$

(C10)
$$\left[-\frac{b^2}{2W^2} + 3\log W\right]_{W_1}^{W_2} = \frac{2\ F/A}{\mu}\ t$$

$$\frac{b^2}{2}\left[\frac{1}{W_1^2} - \frac{1}{W_2^2}\right] + 3\log\frac{W_2}{W_1} = \frac{2\ F/A}{\mu}\ t$$

For round pieces of ice of radius R

(C11)
$$t = \frac{3}{4}\frac{\mu R^2}{F/A}\left(\frac{1}{W_1^2} - \frac{1}{W_2^2}\right) ,$$

while for very long pieces of width b

(C12a)
$$t = \frac{\mu}{F/A}\left[\frac{b^2}{4}\left(\frac{1}{W_1^2} - \frac{1}{W_2^2}\right) + \frac{3}{2}\log\frac{W_2}{W_1}\right] ,$$

in which t is the time required for the water layer to change in thickness from W_1 to W_2 due to surrounding water flowing under the ice.

When $b \doteq W_2 \gg W_1$, which is the case for any deicing situation, Eq. C12 simplifies to

$$t = \frac{1}{4} \frac{\mu A}{F} \frac{b^2}{W_1^2} \qquad \text{(C12b)}$$

in which t is the time to remove the ice.

APPENDIX D

EQUIPMENT AND PROCEDURE FOR MEASURING WATER THICKNESS

Equipment

The ice condenser consists of two copper disks 3 inches in diameter (see Fig. D1). The top plate is 1/4 inch thick with a small lip around its upper edge

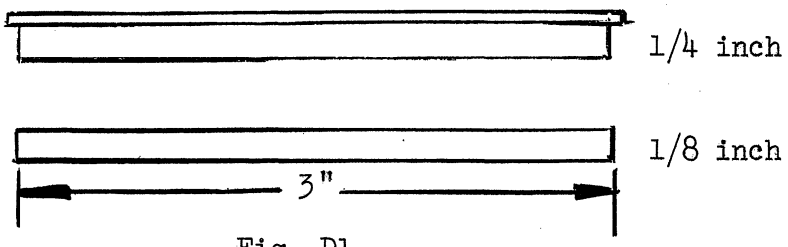

Fig. D1

so that it can be set in its holder. The bottom plate is a plain disk 1/8 inch thick. A wire is soldered to each disk so that an electrical connection can be made with the capacitance change detector. Since the top plate is to be heated uniformly over its surface, its wire is soldered carefully on the lip away from the main body. The placement of the wire on the bottom plate is not critical.

It is important that the top plate be of uniform thickness with a very flat, smooth, unblemished bottom surface to avoid having hot or cold spots appear on the ice during heating. The ice must be melted uniformly over the surface for accurate results.

The jig (Fig. D2) for holding the condenser is a plexiglass disk with a hole in the center the size of the copper disks. Around the hole are cemented three spacers on which the lip of the top copper plate rests. Figure D3 shows how the

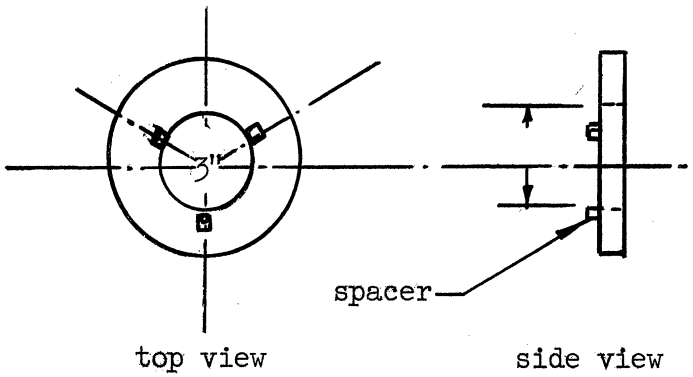

Fig. D2

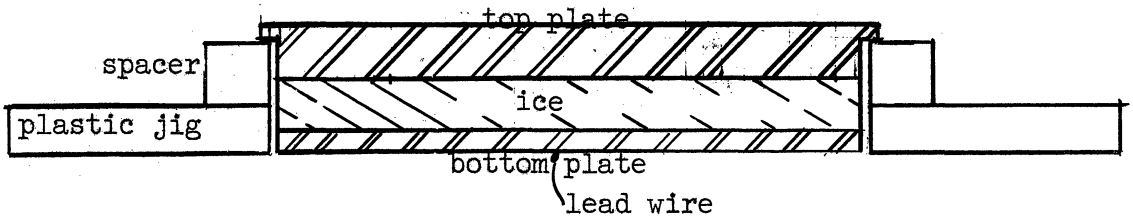

Fig. D3

completed assembly appears after the ice dielectric has been frozen between the plates; the hole in the plastic is just slightly larger than the disk. Note that everything is so dimensioned that the lower plate is still in the hole itself; thus when melting commences the ice and lower plate cannot slip sideways due to any slight tilt of the jig, but are constrained to remain in position by the edge of the hole. This is important in that any slipping would cause a spurious change in capacitance and lead to an erroneous result.

Three components make up the capacitance change detector, a 1.8 mc oscillator, a calibrated variable capacitor in parallel with a potentiometer, and a good vacuum tube voltmeter. The frequency of the oscillator must be above 1.5 megacycles because the dielectric properties of ice are functions of temperature and frequency. Fortunately, however, the dependency of the dielectric coefficient on temperature and frequency decreases as the frequency of measurement increases and at radio frequencies it is effectively constant with respect to both factors. An experiment showed that the dielectric coefficient of ice is constant within 0.75 percent at about 3.0 right up to the melting temperature, while the resistive component decreases linearly with temperature. The 0.75 percent variation is easily accounted for by experimental errors. Thus at this radio frequency an easily discernable discontinuity in dielectric constant occurs precisely at melting.

The variable capacitor and resistor are used for a substitution method of measurement and will be described briefly. The ice condenser can be represented as a pure capacitance, C*, in parallel with a pure resistance, R*, as represented in Fig. D4. Since ice is a poor dielectric, any ice condenser will have a relatively low parallel resistive component. The usual capacity measuring devices are useless in this case because the resistive component is so low compared to ordinary dielectrics. However, a substitution method can be used. The ice condenser is

Fig. D4

loosely coupled inductively to the RF oscillator. Then a calibrated resistor and capacitor are substituted for the ice condenser and adjusted until they give the same response in the oscillator circuit as the ice condenser. The resistance and capacitance must then be equivalent to the ice condenser. Figure D5 shows the three

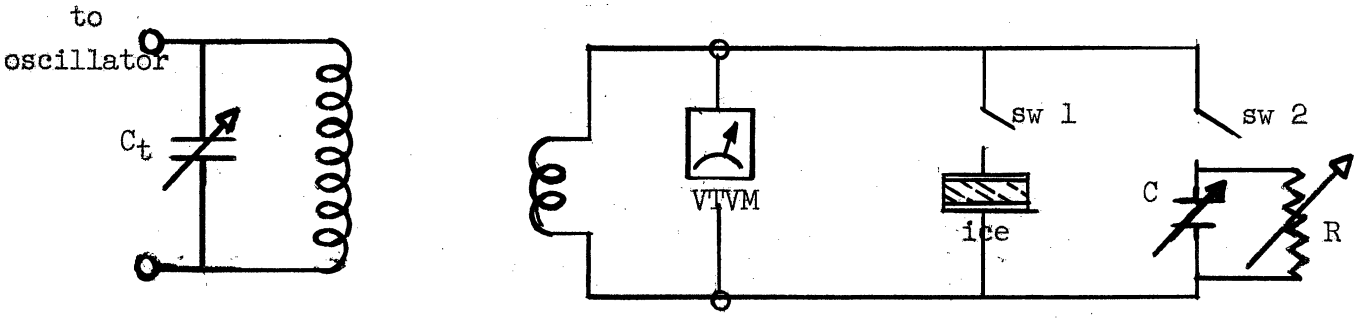

Fig. D5

components pictorially. It is important to calibrate and keep low the capacitance of the leads from the calibrated condenser unit to the ice condenser; other stray capacitance being unimportant as long as it is kept constant during the experiment. A schematic of the capacitance change detector is given in Fig. D11.

A good capacity bridge capable of 5 percent accuracy or better is required to calibrate the variable capacitor since it may be necessary to bias the variable capacitor with a little fixed capacitance at times; depending on the different dielectric thickness being used. A heater capable of uniformity heating the top plate of ice condenser is necessary. An ordinary heat lamp about 6 to 8 inches away from the plate worked quite well. Furthermore, by adjusting this spacing, the melting rate can be increased or decreased. Finally, a deep freeze unit is needed (a) to freeze the ice dielectric to the plates initially and (b) as a cold place in which to conduct the experiment.

Operation

In preparing the ice condenser it is necessary to obtain a thin sheet of ice frozen between two parallel electrodes. It is also necessary that the electrodes remain parallel after melting starts instead of tilting as shown in Fig. D6. The procedure for producing such an ice condenser is to put the electrode which will be heated upside down in a pan of distilled water. Several small chips of insulating material are then placed on the electrode near the periphery. Three or four short pieces of copper wire are placed on the plate with their ends sticking out over the

Fig. D6

edge and the other electrode is set down on the copper wires as shown in Fig. D7. The diameter of the wires thus determines the speacing between the plates, and since

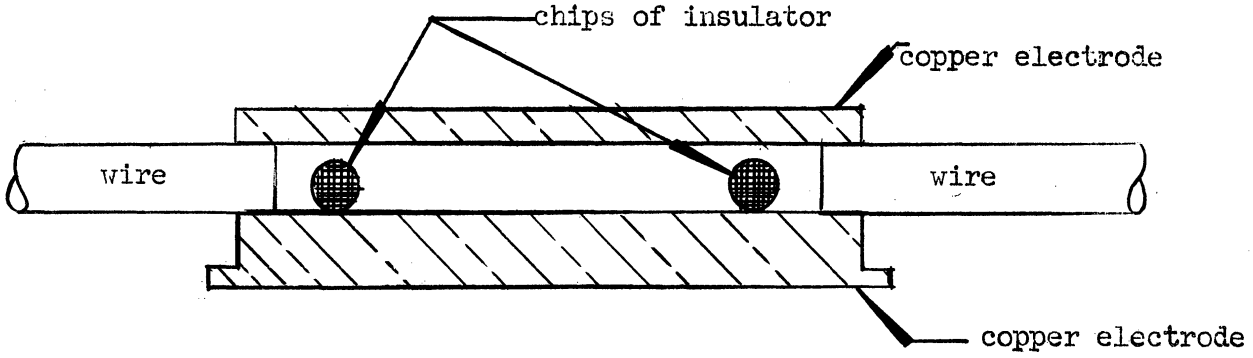

Fig. D7

this can easily be measured it provides a convenient way of determining spacing. The several parts are then lifted out from the water as a unit. If the plates are lifted out horizontally, the water remains between the plates due to the effect of surface tension. With reasonable care, water can be maintained between plates which are separated by as much as 1.5 mm. The assembly is then placed in a freezer and a weight is placed on top of the upper electrode. This weight prevents the water from raising up the top plate as it freezes. After the water has frozen, the wire spacers can be removed by pulling them out with the fingers. The heat from one's fingers is conducted down the copper wire and melts a film of ice surrounding them so that they can be removed very easily. The ice condenser is now ready for test.

The action of the little insulator chips in preventing tilting is illustrated in Fig. D8. After melting starts, the bottoms of the chips are still supported in

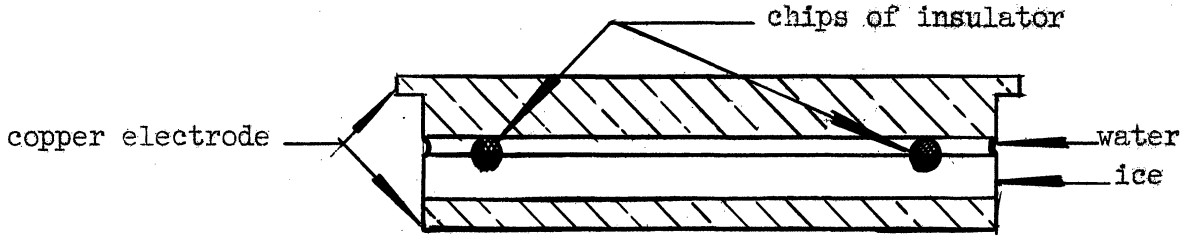

Fig. D8

the ice, but their tops bear against the heated copper surface and prevent it from tipping.

The equipment is set up as shown in Fig. D9 and the initial capacitance, C_o is measured by using the technique of the substitution method. The ice condenser is coupled to the RF oscillator by closing switch 1 and opening switch 2. Next, the oscillator is tuned near resonance as shown by a maximum on the voltmeter and the voltmeter is read. Then the ice condenser is removed from the circuit by opening switch 1 and the resistor and calibrated capacitor substituted by closing switch 2. The C and R are then adjusted to obtain a maximum on the voltmeter at the same voltage as before. C and R must then be equal to C_o and R_o.

The ice condenser, which has been placed in its holder and adjusted so it is horizontal, is loaded with a weight, the weight of the lower plate and the additional weight constituting the total load on the ice. Then the heat lamp is turned on.

The tank condenser C_t in Fig. D5 is continuously adjusted for a maximum reading on the VTVM. When the lower plate falls, the reading on the VTVM just prior is noted and C_t left alone. Next the calibrated condenser and resistor are substituted by throwing a switch and adjusted so the VTVM reads a maximum of exactly the same value noted. The values of C and R must now equal C* and R*. $\Delta C = C^* - C_o$.

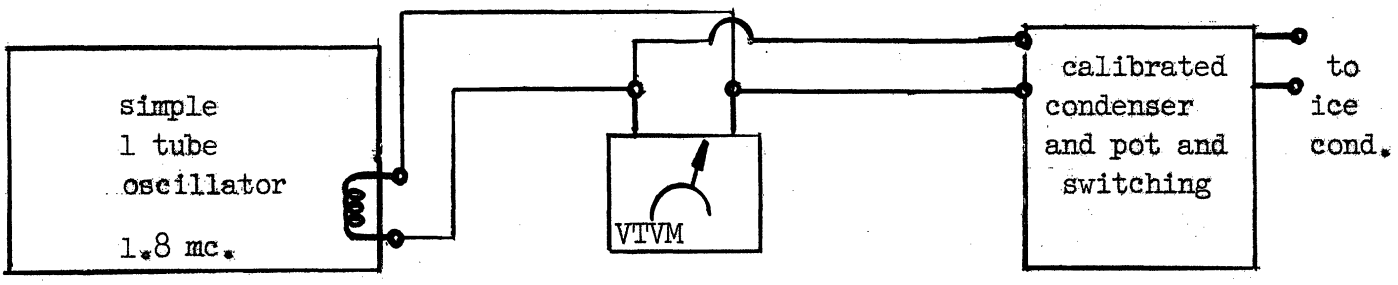

Fig. D9

Knowing C_o, a, and ΔC, the ice melted, x., is computed from the equation,

$$\frac{x}{a} = \frac{\epsilon}{\epsilon - e} \frac{1}{1 + (C_o/\Delta C)} ,$$

where ϵ is the dielectric coefficient of water and e of ice. The deviation is:

$$C_1 = \frac{K\epsilon}{x}$$

K = constant

$$C_2 = \frac{Ke}{a - x}$$

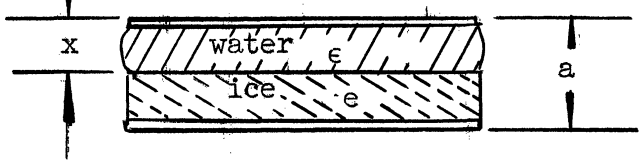

Fig. D10

$$\frac{1}{C} = \frac{1}{C_1} + \frac{1}{C_2} = \frac{x}{K\epsilon} + \frac{a - x}{Ke}$$

$$= \frac{ex + ea - \epsilon x}{K\epsilon e}$$

$$x = \frac{a\epsilon}{\epsilon - e} - \frac{K\epsilon e}{C(\epsilon - e)}$$

When $x = 0$, $C = C_o$ so

$$K = \frac{aC_o}{e}$$

$$\frac{x}{a} = \frac{\epsilon}{\epsilon - e} \frac{C - C_o}{C} = \frac{\epsilon}{\epsilon - e} \frac{1}{1 + (C_o/\Delta C)}$$

Errors in x

The errors inherent in this system manifested by an error in x can be estimated using the previous equation.

$$\frac{x}{a} = \frac{1}{1 + \frac{C_o}{\Delta C}} \cdot \frac{\epsilon}{\epsilon - e}$$

$$\frac{dx}{x} = \frac{da}{a} + \frac{e}{\epsilon - e}\left(\frac{de}{e} - \frac{d\epsilon}{\epsilon}\right) + \frac{C_o}{C_o + \Delta C}\left(\frac{d\Delta C}{\Delta C} - \frac{dC_o}{C_o}\right)$$

The factor $e/\epsilon - e$ is small. Therefore the dielectric coefficients of ice and water need be known only approximately. This explains why no determination of them was made. The usual values of 3 and 81, respectively are sufficiently accurate. Neglecting errors in the dielectric the equation reduces to

$$\frac{dx}{x} = \frac{da}{a} + \frac{C_o}{C_o + \Delta C}\left(\frac{d\Delta C}{\Delta C} - \frac{dC_o}{C_o}\right) .$$

An estimate can now be made of the total error.

$$\frac{da}{a} = 5\% \qquad \text{(error in determining wire size)}$$

$$\frac{d\Delta C}{\Delta C} = 5\%$$

$$\frac{dC_o}{C_o} = 5\% \quad .$$

Since $\frac{C_o}{C_o + \Delta C}$ was about .7 the total error is about 7%.

A calculation of the thermal expansion of ice showed that its effect on the capacitance of the ice condenser is insignificant.

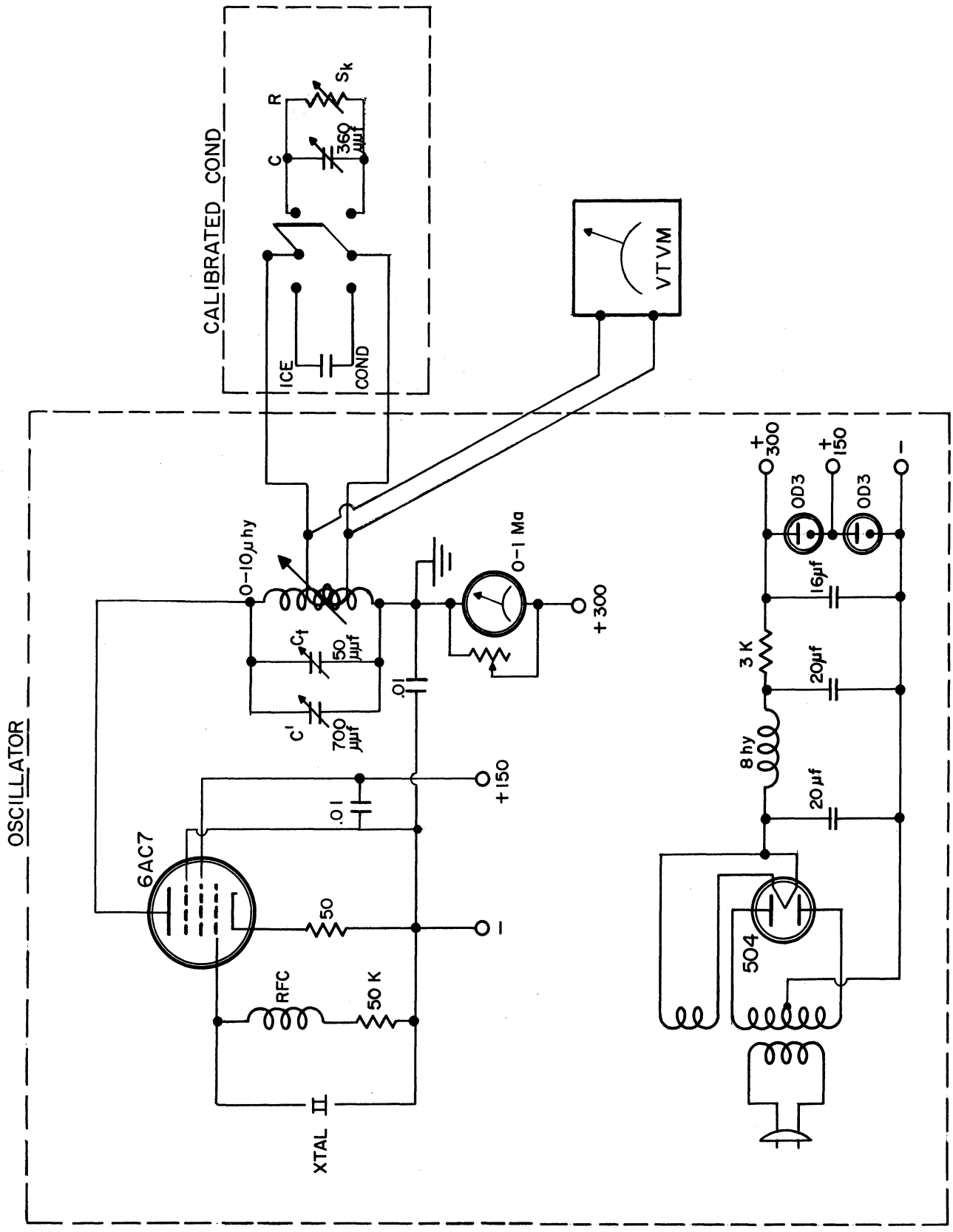

Fig. D11. Schematic of Capacitance Change Detector.

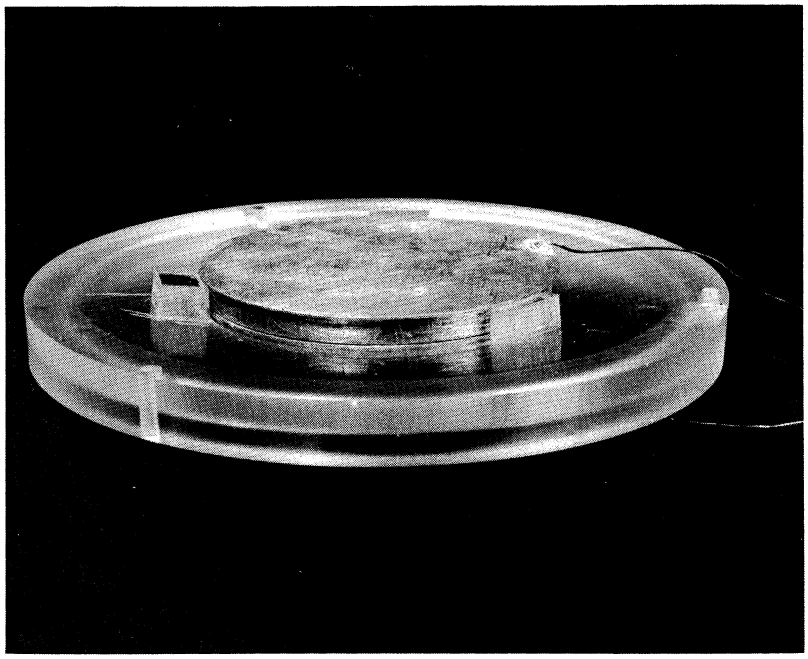

Fig. D12. Close-Up of Ice Condenser in Its Holder.

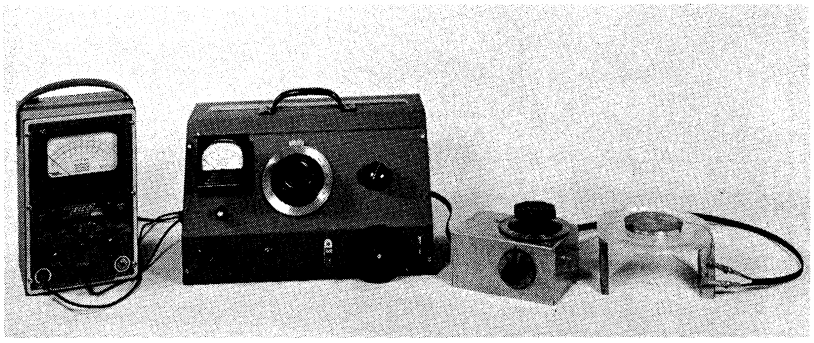

Fig. D13. Capacitance Change Detector.

APPENDIX E

DEVELOPMENT OF A TECHNIQUE FOR THE FABRICATION OF MODELS CAPABLE OF DELIVERING APPROXIMATELY 100 PERCENT OF THE GENERATED HEAT AT THE SURFACE FOR THE EXPERIMENTAL INVESTIGATION OF INTERMITTENT DEICING

At the beginning of this investigation the various types of models being used by investigators in the field of heat transfer were considered for possible adaptation to this experimental program. A model was desired capable of dissipating high power densities at the surface. At the same time, surface temperature measurements were desired at a number of points over the surface in order to correlate analytical results with experimental data for the deduction of the amount of ice melted at the time shedding takes place. Nichrome ribbon heaters bonded to the model surface appeared to be the most common method of model construction and the most suitable for the high intensities desired. However, difficulties experienced with bonding the nichrome ribbon to the model surface and at the same time avoiding surface imperfections resulted in a search for a better technique. Conductive carbon coatings applied to plastic models which had thermocouples imbedded 0.005 inch from the surface were tried and found to be quite successful for heat transfer studies at a low intensity level up to 10 watts/in^2. This was considered insufficient to carry out the experimental program desired, and the search for a better coating was continued. It was discovered that "Silver Paint," a product of the General Cement Company and used for printed circuits, could be used as a conductive coating capable of very high heat and generating capacities limited only by the temperature limit of the coating around 300 to 400°F. (Dupont Company makes a paste which can be diluted with amyl alcohol to perform the same function.) Pastic models were again tried, but model failure occurred from burnout at the high intensities, due to local hot spots which formed since the uniformity of the coating was of the order of $\pm$ 10 percent. It was decided that a model consisting of a poor conductor for a base covered with a thin copper foil would eliminate this problem. A 6-inch balsa airfoil (NACA65$_2$-016) was fabricated and a copper foil .005 inch thick, which had thermocouples spotwelded to the inner surface, was bonded to it with Cox's* heating element adhesive No. 28. Slots .005 inch deep were milled at 3/4 inch intervals around the airfoil to within 1/2 inch of the edge.

The entire surface of the foil was then coated with a thin plastic film and baked to insulate it electrically. The silver paint was applied to each strip separately by spraying, maintaining electrical insulation between the strips with masking tape at the time of application of this paint. Two coats of paint were required, each coat baked one-half hour at about 200°F. Bus bars and lead wires were attached at each end of the heater strips by screwing copper bars down onto the silver paint using plastic shims to isolate the screws from the copper bases. This completed the fabrication of the model; then all elements were checked for electrical isolation from each other as well as from the copper base.

The finished model was placed in the University of Michigan Icing Wind Tunnel and preliminary tests indicated that it was capable of delivering the desired

*Cox and Co., New York, N. Y.

intensities without burnout. The initial tests also indicated that consistent shedding result could not be obtained, due to bonding of the ice at the edges of the model. This was remedied by the installation of guard heaters at the edges. The performance of the model in this form was highly satisfactory. Power densities up to 43 watts/in.^{2} were obtained. No higher densities were tried due to the short time intervals required for shedding at this point. These tests are discussed in the body of this report as Test Series F.

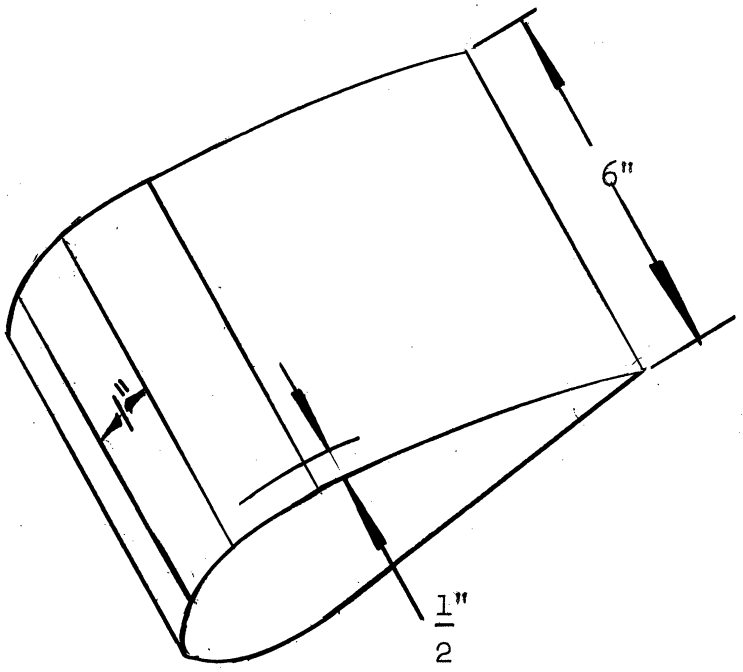

Fig. E1.

APPENDIX F

MISCELLANEOUS NOTES

The following two notes are included as matters of some interest which are not directly related to the main subject matter of this report.

A series of tests were initiated wherein it was intended that heating rates approaching 1000 watts/in.^{2} would be used. The areas of particular interest in this phase were:

1. Establishment of the minimum amount of energy required to remove the ice for a particular system,

2. determine if the mechanism of removal might change radically at high heating rates, and

3. establish the effect of heating rates on the thickness of the water layer.

A number of flat rectangular elements, consisting essentially of brass shim-stock attached at the ends to copper buss bars, were assembled in a walk-in cold storage room held at about 15 $\pm$ 2°F.

After freezing a block of ice to the heating elements and allowing time for cooling of the element to room temperature (+ 15°F), the desired voltage was applied to the element.

A very slight spring loading on the block of ice caused it to be displaced, after sufficient melting had occurred, and to engage a micro switch which shut off the applied voltage. The voltage and amperage were recorded on an oscillograph. Several difficulties and a few conclusions resulted from these tests.

1. Extreme care was required in attaching the ice block by freezing to the heating element uniformly and with no overhang on any side.

2. As the heating rate was increased and the ice released more rapidly, the amount of time required for the ice to move sufficiently to interrupt the power became a larger percentage of the power on time. That is, a tare, presumed to be roughly constant, of unknown quantity was included in each run; thus indicating higher total energies than was actually required to free the ice.

3. Heating rate of over 100 watt/in.^{2} were employed for this first series under conditions described above. The total energy required for removal appeared to have almost reached a minimum, for this system, of about 4-1/2 watt sec/in.^{2} at rates of 125 watt/in.^{2}.

4. Calculations were made of the average water film thickness using the simplifying assumption that all the energy went into either heating the element or melting the film of ice. The values obtained varies from .0006 to .00198 in. with the thinner layers resulting from the higher heating rates. This would necessarily follow under the assumptions made for these calculations.

Because of the tare mentioned above, a number of tests were made at increased heating rates wherein the power on time was pre-set for each trial and the success or failure of the test recorded as well as volts and amps. The thought being that the time required to just barely remove the ice with a given applied voltage would establish the minimum time and energy for that voltage. Unfortunately, difficulties in recording the data and apparent discrepancies in the results were such that a modified recording and control system would be necessary before useful data at higher heating rates could be recorded. Heating rates approaching 1000 watt/in.^{2} were supposedly used, but inaccuracies in the data left some question as to the actual heating rate reached. At these higher rates the ice appeared to be freed from the model instantaneously. The program was discontinued at this stage mainly because of increased emphasis in other areas of deicing. With proper models and recording techniques it appears that further tests at heating rates in excess of 100 watts/in.^{2} should produce interesting and meaningful data.

Ice Characteristics

From a very few samples of ice collected from aircraft in flight it was found that the ice differed little from ordinary ice. However, the grain structure was very uniform and the C axis of the crystals was normal to the surface.

More samples were not collected because the authorization for collection came very late in the icing season.

DATA FOR TEST SERIES A

Plotted on Fig. 13

a	C_o	ΔC	Δa	P
.0865 cm	202 μμF	173 μμF	.0415 cm	2.65 gm/cm^2
.0865	194	234	.0485	
.0865	202	177	.0420	
.0865	197	169	.0420	
.0865	200	196	.0445	
			Avg. .0437	
.0865	198	125	.0345	3.75 gm/cm^2
.0630	255	298	.0350	
.0865	201	132	.0355	
			Avg. .0350	
.0600	258	150	.0230	4.85 gm/cm^2
.0600	256	145	.0230	
.0600	259	161	.0235	
			Avg. .0232	
.0600	257	127	.0210	5.96 gm/cm^2
.0600	262	131	.0205	
.0600	259	119	.0195	
			Avg. .0203	
.0600	264	64	.0125	13.7 gm/cm^2
.0600	263	93	.0160	
.0600	262	66	.0125	
.0600	246	65	.0135	
.0600	257	76	.0143	
			Avg. .0137	
.0865	208	345	.056	2.13 gm/cm^2
.0865	208	281	.052	
			Avg. .054	

DATA FOR TEST SERIES B AND C

Plotted on Fig. 8

Test	Test Data				Water Melted (gm)	Area (cm^2)	U_o/ϕ	t_o (sec)	W_B (cm)	W_C (cm)	t/t_o	$\rho LW/\phi t_o$	
	U_o (°C)	ϕ (cal-cm^{-2}-sec^{-1})	$t + t_o$ (sec)	Force (gm)								B	C
A	-25	.145	83	32		25.8	172	56.7	.112		.482	1.09	
B	-26	.142	80				183	64.2			.246	.983	
C	-23	.146	73				158	47.9			.524	.916	
D	-24	.685	16				34.9	2.33			5.87	5.61	
E	-24	.685	19				35.0	2.35			7.085	5.57	
F	-24	.639	14				37.6	2.71			4.166	5.18	
G	-24	.583	21				41.1	3.24			5.05	6.86	
H	-24	.627	17				38.3	2.81			4.88	5.09	
I	-25	.645	17				38.8	2.89			4.88	4.81	
J	-25	.607	19				41.2	3.26			4.83	4.53	
K	-23	.655	2	86		19.75	35.1	2.36	.033			1.71	
L		.655	3	86			35.1	2.36	.033		.271	1.71	
M	-23	.649	16	36			35.4	2.40	.077		5.67	3.96	
N	-24	.363	32				66.0	8.35			2.83	2.03	
O	-25	.398	44.5				67.8	8.80			4.06	1.76	
P	- 8	.279	8.55				28.6	1.57			4.45	14.0	
Q	- 8	.267	19.25				29.9	1.71			10.26	13.5	
R	- 8	.275	21.0	35.0	.9		29.1	1.62	.079	.0456	11.96	14.2	8.19
S	-13	.266	26.0	36.2	1.0		48.9	4.58	.076	.0507	4.68	5.88	3.70
T	-13.2	.266	23.3	35.6	.7		49.7	4.73	.077	.0355	3.93	4.90	2.26
U	-13	.251	22.95	36.7	.6		51.8	5.15	.075	.0304	4.04	4.64	1.88
V	-15	1.265	4.87	35.5	.55		11.87	.27	.077	.0278	17.04	18.1	6.50
W	-16	1.185	5.24	35.35	.75		13.5	.35	.077	.0380	13.97	14.9	7.36
X	-14	1.22	3.08	69.8	.8		11.47	.252	.047	.0405	11.3	12.25	10.55
Y	- 6.2	1.24	2.14	70.3	.7		5.01	.0482	.040	.0355	43.58	53.5	47.5
Z	- .8	1.19	2.8	69.1	.7		6.71	.0864	.041	.0355	31.4	31.9	27.6
AA	-10.6	.598	4.67	69.9	.5		17.7	.600	.0405	.0253	6.8	9.01	5.64
AB	-10.7	.451	6.70	70.6	.25		23.2	1.030	.0395	.0127	5.50	6.8	2.19
AC	- 1.2	.587	1.53	35.3	.5		2.045	.800	.077	.0253	18.12	13.1	4.31
AD	- 2.5	.587	6.22	35.8	1.1		4.27	.035	.076	.0557	177	296	217
AE	- 3	.560	7.05	33.6	.72		5.35	.055	.082	.0364	127	213	94.6
AF	- 1.5	.605	6.23	35.9	.93		2.48	.0118	.077	.0471	527	864	528
AG	0	.280	17.76	35.7	.52		0	0	.078	.0263			
AH	- 4.5	.284	17.85	34.7	.65		15.84	.481	.080	.0329	38.6	37.8	19.3
AI	- 1.5	.275	12.97	37.1	.7		5.45	.057	.075	.0354	226	383	181

CALCULATIONS FOR TESTS OF SERIES D

Plotted on Fig. 11

Test	U_o	ϕ	$t + t_o$	F	U_o/ϕ	t_o	t/t_o	S	J	St_o/J
AK	-17.2	.629	12.75	35	27.3	.295	42.2	34.5	1.55	6.56
AL	-12	.617	1.79	35	19.45	.084	20.3	15.5	1.57	.76
AM	- 8.4	.604	2.60	35	13.9	.076	33.2	27.0	1.60	1.28
AN	- 8.6	.259	5.56	38	33.2	.435	11.78	8.4	2.74	1.34

$\rho L = 79.71$

$$\mu Ab^2 = \frac{(.01794)(19.75)(1.75)^2}{980}$$

But this is for long narrow pieces use $\left(\frac{3}{4} b^2\right)$ in place of b^2

$$\therefore \mu Ab^2 = \frac{(.01794)(19.75)(1.75)^2(.75)}{980} = 8.30 \cdot 10^{-3}$$

Test	ϕ	F	$\frac{\rho L}{\phi}$	$\frac{\mu Ab^2}{F}$	J	K	t/J	$\frac{.6}{k}$
AK	.629	35	120.7	$.237 \cdot 10^{-3}$	1.55			
AL	.617	35	129.1	$.237 \cdot 10^{-3}$	1.57			
AM	.604	35	132.0	$.237 \cdot 10^{-3}$	1.60			
AN	.259	38	308.0	$.219 \cdot 10^{-3}$	2.74			

CALCULATIONS FOR SERIES E

Use $\left(\frac{v}{V}\right)^2$ from 65_2 - 015 airfoil in NACA Rept. 824

% C	13.3	20	Ave.
$\left(\frac{v}{V}\right)^2$	1.318	1.374	1.346

$\frac{1}{2}\rho V^2$ = .0821 psi at 100 fps

$\Delta\rho_{air}$ = 1.346 (.0821) = .1104 psi = 7.57 $\frac{gm}{cm^2}$

$W_{req} = \frac{2\gamma}{\Delta\rho_{air}} = \frac{2(.000432)}{.1104}$ = .00782"

= .01987 cm

DATA FOR TEST SERIES E

Test	V_o	ϕ	$t + t_o$	V_o/ϕ	t_o	t/t_o	S
AP	-16.1	.374	12.86	43.1	3.6	2.57	1.27
Q	-16.1	.233	27.2	69.2	9.2	1.96	.90
R	-16.1	.368	14.7	43.8	3.8	2.87	1.47
S	-16.1	.368	17.0	43.8	3.8	3.47	1.87
T	-16.1	.385	13.0	41.9	3.4	2.82	1.45

	$\frac{\rho L}{\phi}$	$\left(\frac{\rho L}{\phi}\right)^{1/3}$	$\frac{\mu A b^2}{F}$	$\left(\frac{\mu A b^2}{F}\right)^{1/3}$	k	J	W/k	$\frac{t_o S}{J}$
AP	213	5.96	$4.81 \cdot 10^{-6}$		.00224	.598	8.86	7.63
Q	342	6.99		.01685	.00191	.823	10.38	10.06
R	217	6.00			.00223	.607	8.90	9.2
S	217	6.00			.00223	.607	8.90	11.70
T	207	5.91			.00226	.588	8.78	9.37

corrected by using F/A = .0774 psi = 5.30 $\frac{gm}{cm^2}$

W = .0284 cm

	$\frac{t_o S}{J}$	k	$\frac{W}{k}$
AP	6.77	.00253	11.20
Q	9.40	.00216	13.13
R	8.15	.00251	11.30
S	10.15	.00251	11.30
T	8.31	.00255	11.13

DATA FOR TEST SERIES F

Heater area .70" x 4.5"
from NACA 65_2 - 015 aerofoil

PRESSURE ESTIMATES (Linear interpolation)

% C	1.67	11.67	Ave.
$\frac{v}{V}^2$	.980	1.299	1.140

use 1.140 $\frac{1}{2}\rho U^2$

$V = 230$ fps

$\frac{1}{2}\rho V^2 = .435$ psi

$1.140\ (.435) = .496$ psi

$= 34.9\ gm/cm^2$

TEST SERIES F_1

Test	Watts / in.^{2}	Time Shed	Time No shed	$\frac{\rho L}{\phi}$	$\left(\frac{\rho L}{\phi}\right)^{1/3}$	$\frac{W}{k}$	J	t/J shed	t/J no shed
FA	1.	20	15	2150	12.89	11.29	1.055	19.0	14.2
FB	1.25	18	15	1720	11.97	10.48	.910	19.8	16.5
FC	2.5	4.5	4.0	860	9.50	8.33	.574	7.83	6.97
FD	3.5	4	3.5	615	8.50	7.45	.459	8.71	7.63
FE	4.5	4	3.5	478	7.87	6.90	.393	10.2	8.9
FF	4.75	3.5		452	7.67	6.72	.373	9.4	
FG	6.5	2.9	2.0	231	6.13	5.38	.239	12.1	8.4
FH	12.5	3.0	2.5	172	5.55	4.86	.196	15.3	12.8
FI	22	2.0*	1.0	97.7	4.60	4.03	.1345	14.9	7.4
FJ	44	1.0	.5	48.9	3.65	3.20	.0847	11.8	5.9

*sliding back

$$\frac{\mu A b^2}{F} = \frac{.01794(.70)^2}{980\ (34.9)} = .257 \cdot 10^{-6}$$

$$= (.00635)^3$$

$$k = \frac{.00504}{\left(\frac{\rho L}{\phi}\right)^{1/3}}$$

$$J = .00635 \left(\frac{\rho L}{\phi}\right)^{2/3}$$

$$W = \frac{2\gamma}{\Delta P} = \frac{2(75.6)}{980(34.9)} = .00443$$

$$\frac{W}{k} = .877 \left(\frac{\rho L}{\phi}\right)^{1/3}$$

TEST SERIES F_2

Test	$\frac{\text{Watts}}{\text{In.}^2}$	vel. fps	t	ϕ	$\frac{F}{A}$	$\frac{\rho L}{\phi}$	$\left(\frac{\rho L}{\phi}\right)^{1/3}$	$\left(\frac{\mu Ab}{F}\right)$	$\left(\frac{\mu Ab^2}{F}\right)^{1/3}$
FK	1	83	7	.037	4.53	2150	12.90	$1.98 \cdot 10^{-6}$	.01253
L	1	145	11.5	.037	13.8			$.65 \cdot 10^{-6}$	.00865
M	1	230	20	.037	34.9			$.257 \cdot 10^{-6}$	.00635
N	4.8	82	1.5	.178	4.53	448	7.65	$1.98 \cdot 10^{-6}$	.01253
O		142	2.7	.178	13.3			$.675 \cdot 10^{-6}$	.00876
P		230	3.5	.178	34.9			$.257 \cdot 10^{-6}$	.00635
Q	8.3	142	2	.307	13.3	259	6.37	$.675 \cdot 10^{-6}$	.00876
R		230	3	.307	34.9			$.257 \cdot 10^{-6}$	.00635
S		230	1	.307	34.9			$.257 \cdot 10^{-6}$	.00635

	J	t	t/J	k	W	W/k
FK	2.09	7	3.35	.000772	.0341	44.1
L	1.44	11.5	8.0	.000533	.01118	21.0
M	1.057	20	18.9	.000391	.00442	11.30
N	.735	1.5	2.04	.001300	.0341	26.3
O	.513	2.7	5.26	.000909	.01160	12.75
P	.372	3.5	9.41	.000659	.00442	6.70
Q	.355	2	5.62	.001092	.01160	10.60
R	.258	3	11.62	.000792	.00442	5.58
S	.258	1	3.88	.000792	.00442	5.58

SOME PROPERTIES OF WATER AND ICE

		Water (32°F)	Ice (32°F)
Weight	$\frac{lb}{ft^3}$	62.41	57.50
	$\frac{gm}{cm^3}$	.97	.92
Specific Gravity, ρ		1.0	.92
Specific Heat	$\frac{Btu}{lb°F}$	1.00	(.504)
C	$\frac{cal}{gm°C}$	1.00	(.504)
Thermal Conductivity	$\frac{Btu}{hr\ ft\ °F}$	.348	1.294
K	$\frac{cal}{sec\ cm°C}$	1.44×10^{-3}	5.35×10^{-3}
Thermal Diffusivity	$\frac{ft^2}{hr}$	.0066	.0456
α	$\frac{cm^2}{sec}$	1.69×10^{-3}	11.8×10^{-3}
Latent Heat L	$\frac{Btu}{lb}$ cal/gm		144 (heat of fusion) 80
Viscosity	(1 atm) poise	0.01793	

Conversion factors:

1 Btu = 252 cal = 1055 joules = 775 ft lb
1 Watt = .2389 cal/sec = 3.413 Btu/hr
1 lb = 453.6 gm

REFERENCES

1. Carslaw, H. S. and Jaeger, J. C., Conduction of Heat in Solids, Oxford University Press, London, 1947, p. 227-228.

2. Churchill, R. V., Modern Operational Mathematics in Engineering, McGraw-Hill, New York, 1944, (a) p. 106-109, (b) p. 117, problem 4.

3. Evans, Isaacson, and MacDonald, "Stefan-like Problems," Quarterly of Applied Mathematics, VIII, No. 3, 313-314.

4. Landau, H. G., "Heat Conduction in a Melting Solid," Quarterly of Applied Mathematics, VIII, No. 1, 84-94.

5. Langmuir, I. and Blodgett, K. B., A Mathematical Investigation of Water Droplet Trajectories. AAF Technical Report 5418.

6. Messinger and Bernard L., "Equilibrium Temperature of an Unheated Icing Surface as a Function of Air Space," Journal of the Aeronautical Sciences, January, 1953. Also, Energy Exchanges during Icing, Lec. No. 6, University of Michigan Airplane Icing Information Course.

7. Paterson, S., "Propagation of a Boundary of Fusion," Proceedings of the Glasgow Mathematical Society, I, 42-47.

8. Sherman, P., Klein, J. S., and Tribus, M., Determination of Drop Trajectories by Means of an Extension of Stokes' Law, Engineering Research Institute Project 1992, University of Michigan, April, 1952.

9. Stefan and J. Stizber, Akad. Wiss., Wien (Math.-Naturw. Klasse) 69, 713 (1874).

10. Tribus, M. and Rauch, L. L., A New Method for Calculating Water Droplet Trajectories about Streamlined Bodies, Engineering Research Institute Project 1992, University of Michigan, December, 1951.

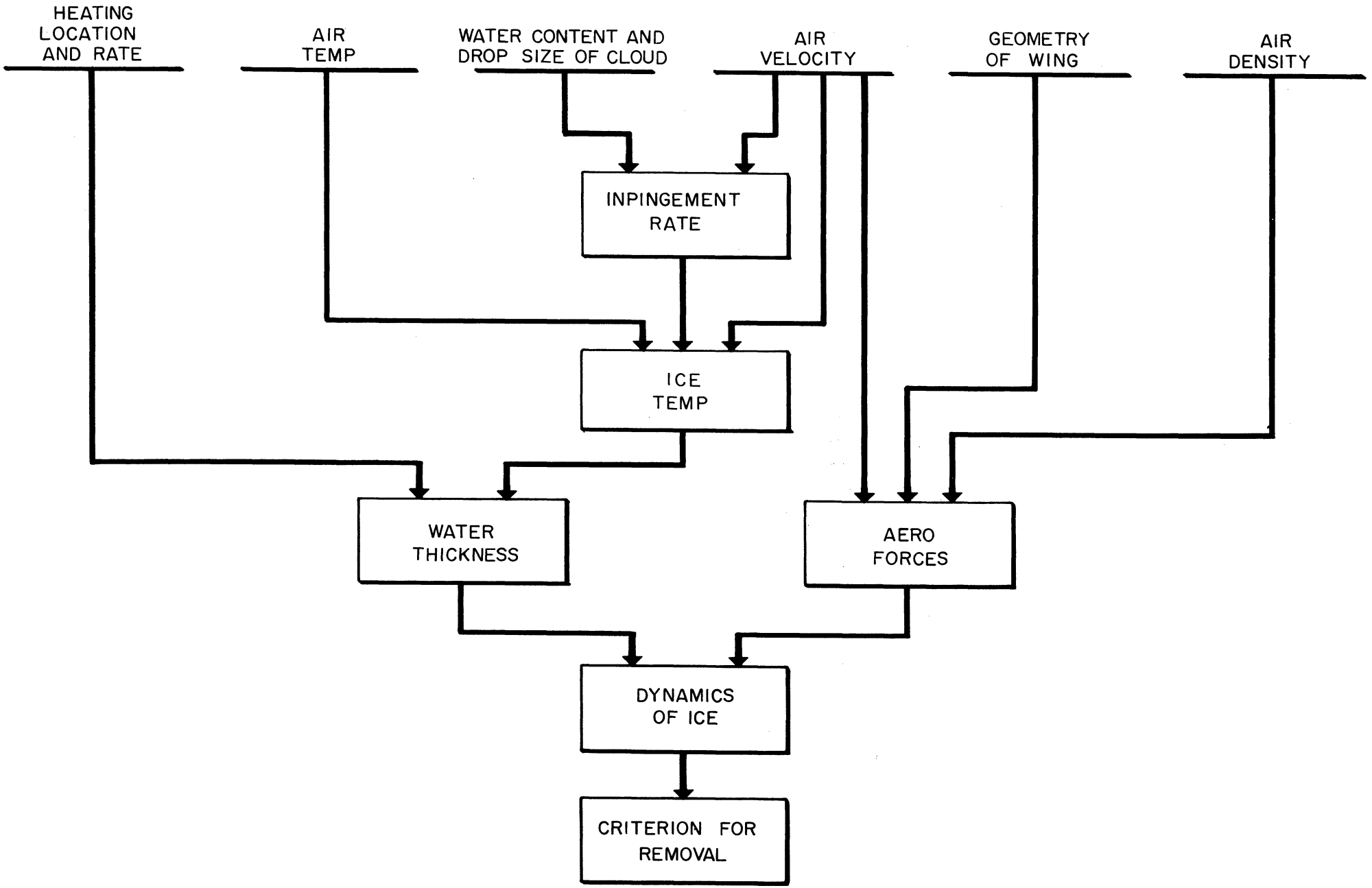

Fig. 1. Schematic of Ice Removal Criterion.

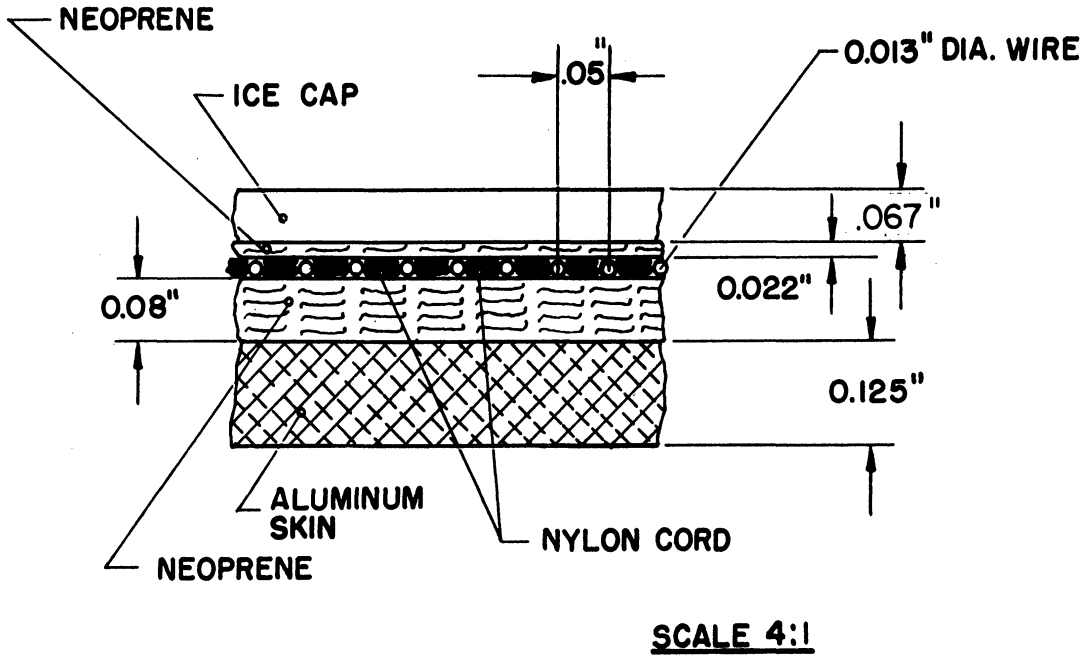

Fig. 2. Dimensions of Rubber Boot.

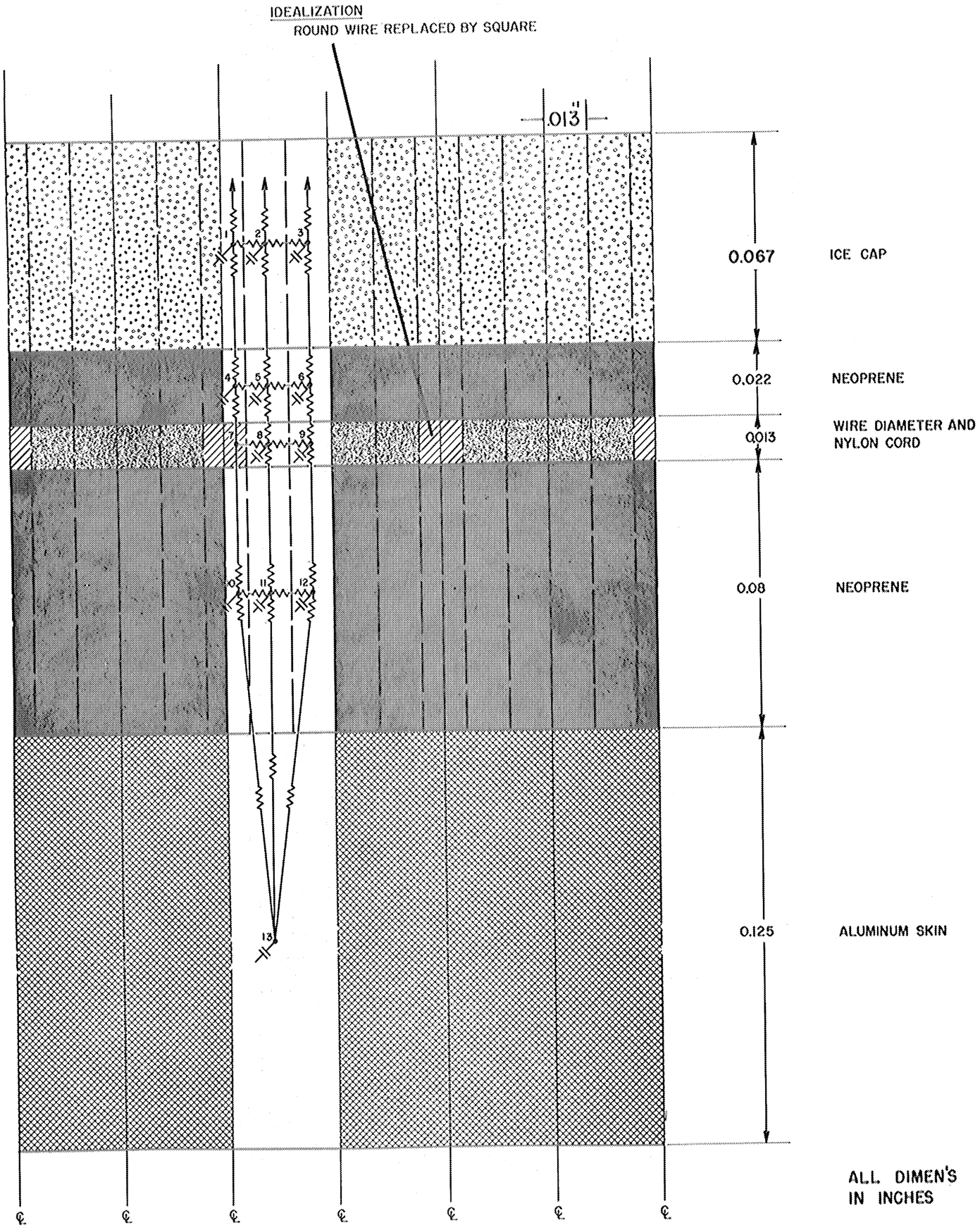

Fig. 3. Idealization of Heater Boot Showing Division of Boot into Cells and Equivalent Electrical Network Superposed.

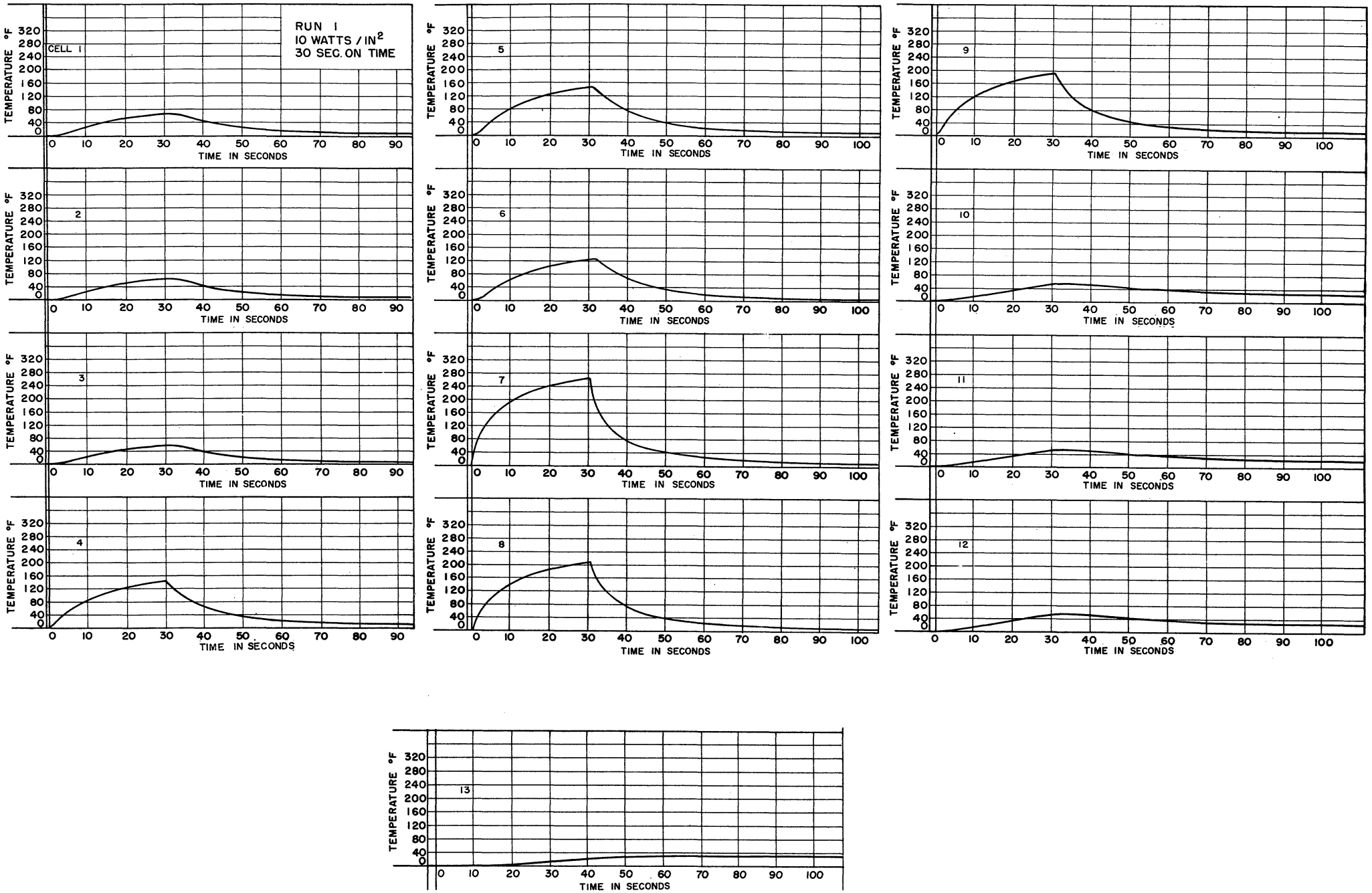

Fig. 4. Cell Temperatures of the Idealized Heater Boot as a Function of Time During a Typical Run.

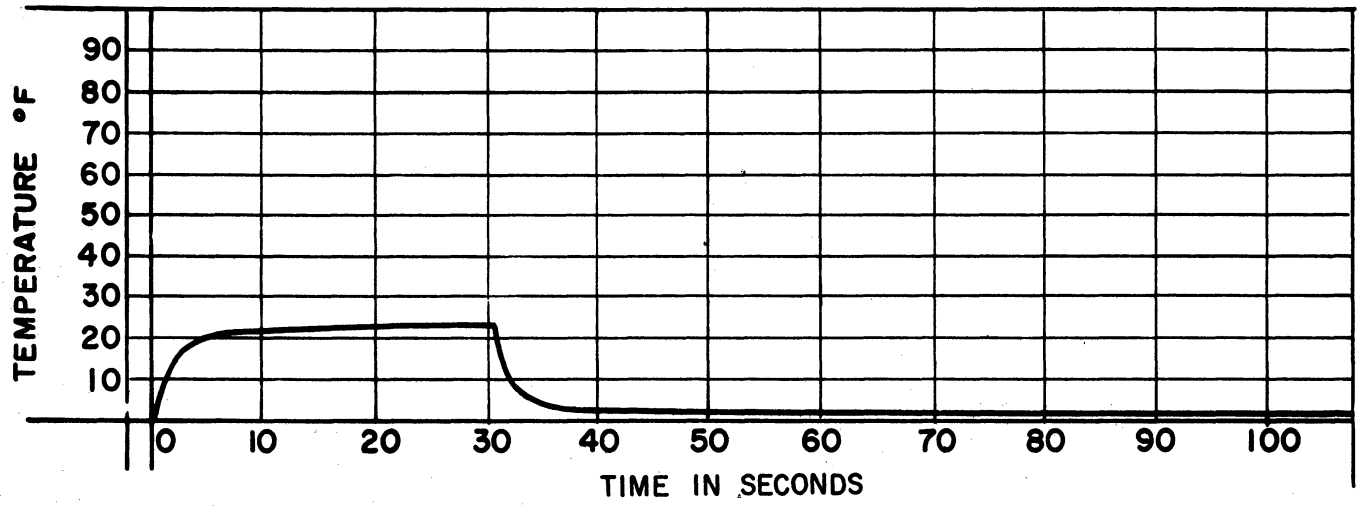

Fig. 5. Temperature Difference between Cells 4 and 6.

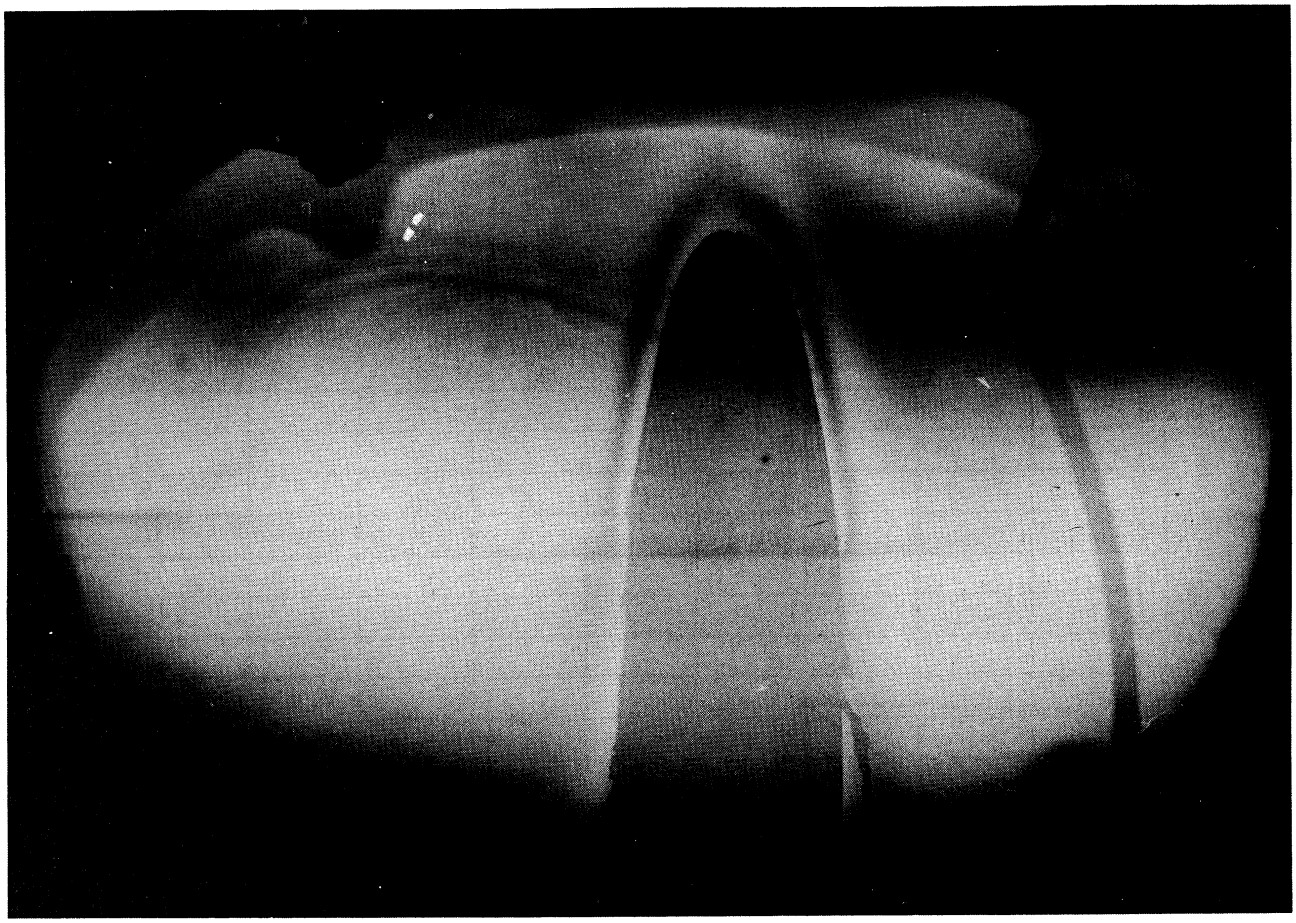

Fig. 6. Interferogram of Boot Two Seconds after Power is Turned On - All Wires Energized.

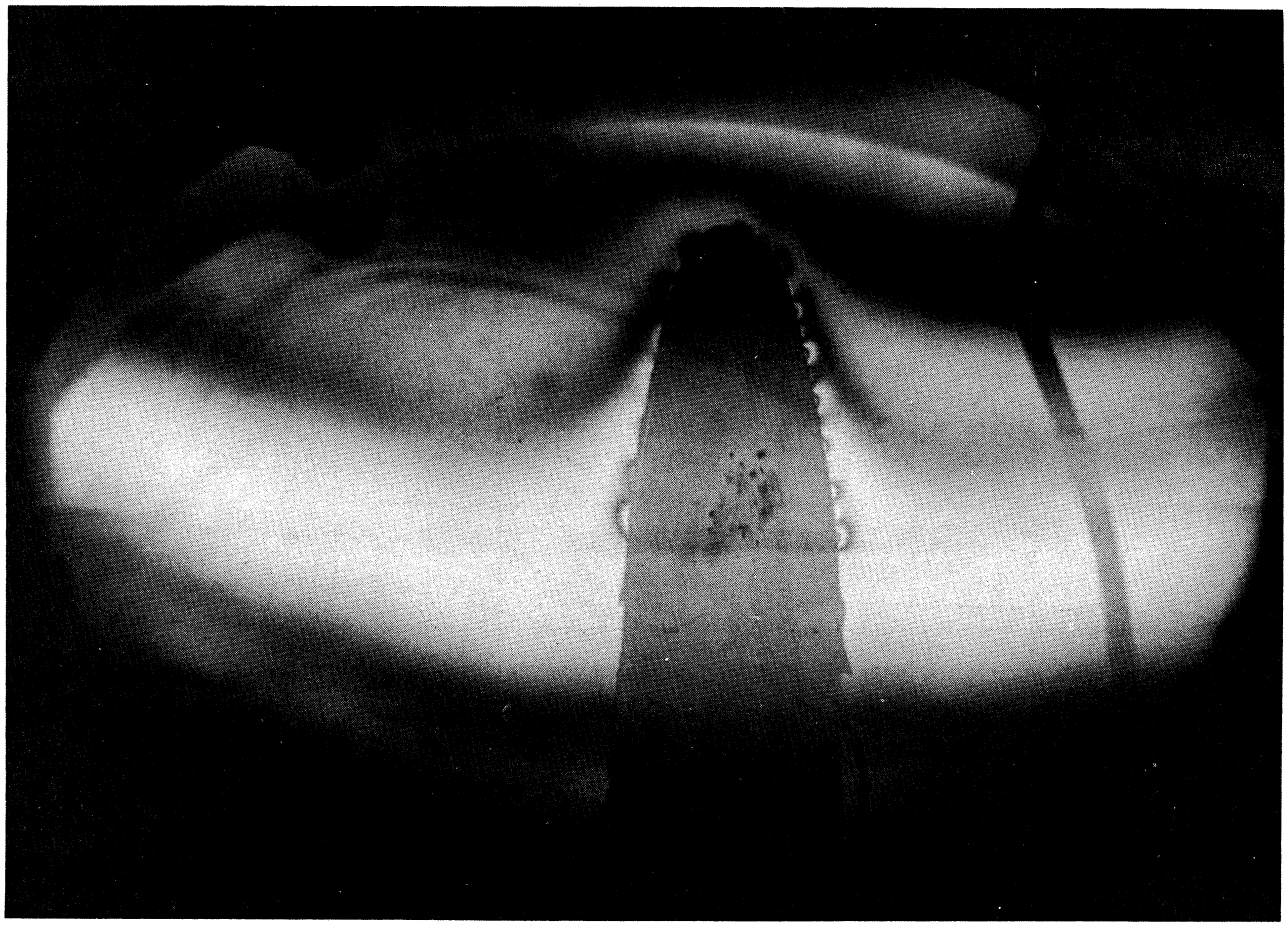

Fig. 7. Interferogram of Boot 2 Seconds after Power is Turned On - Half of Wires Energized.

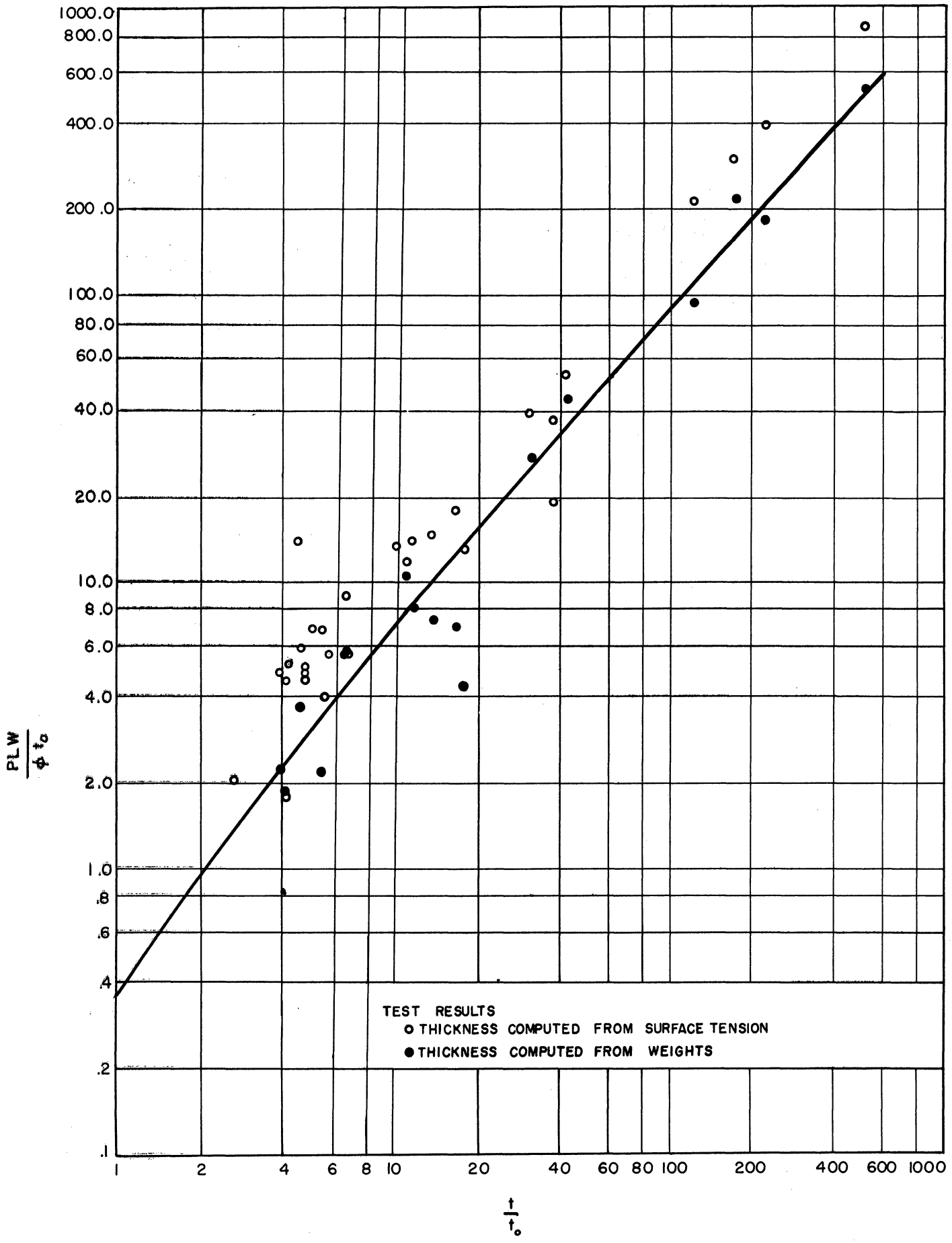

Fig. 8. Comparison of Theoretical and Experimental Melting Rate.

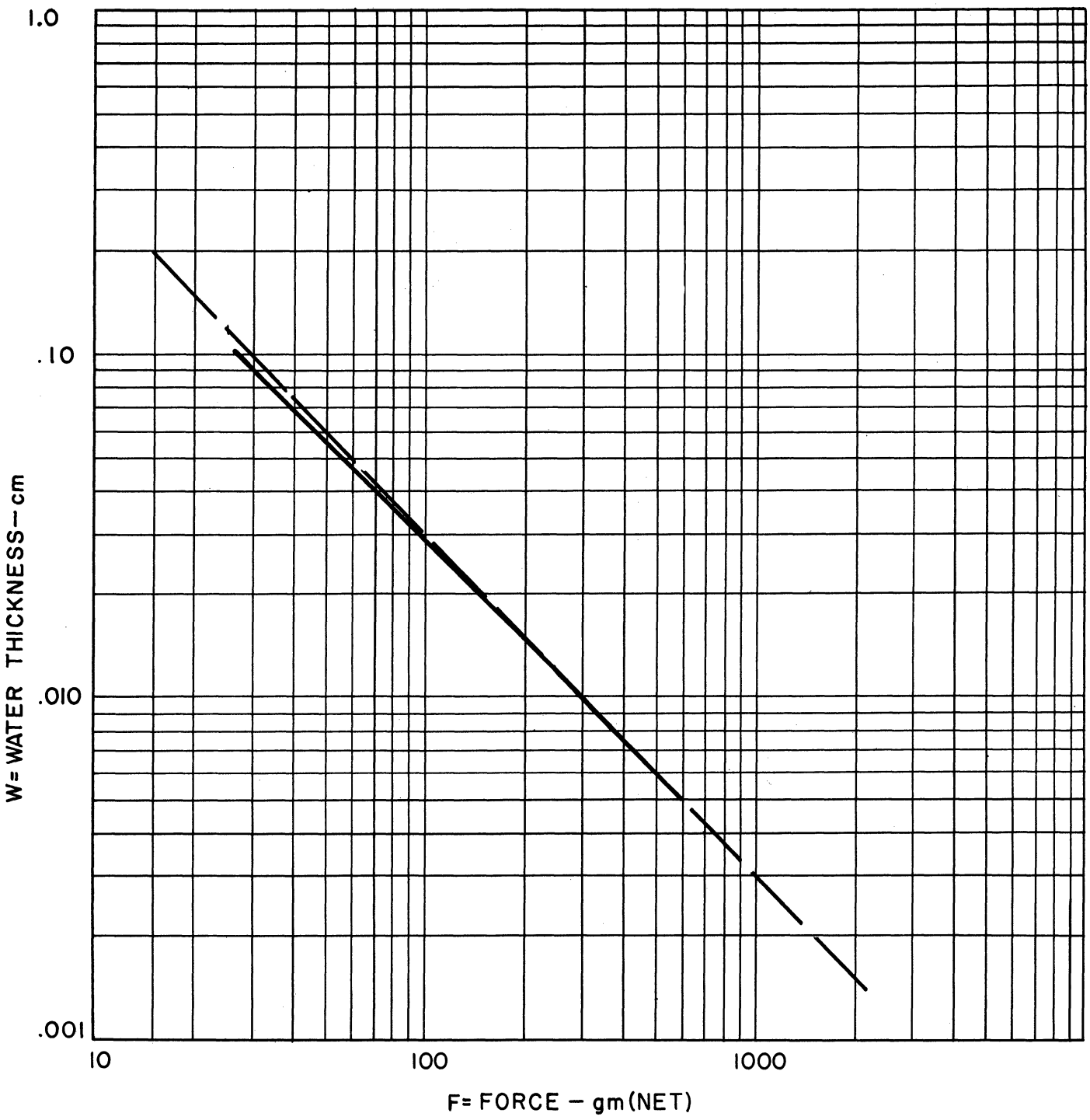

Fig. 9. Force (gm) Thickness (cm) Relation for 1.75" Square with No Excessive Water.

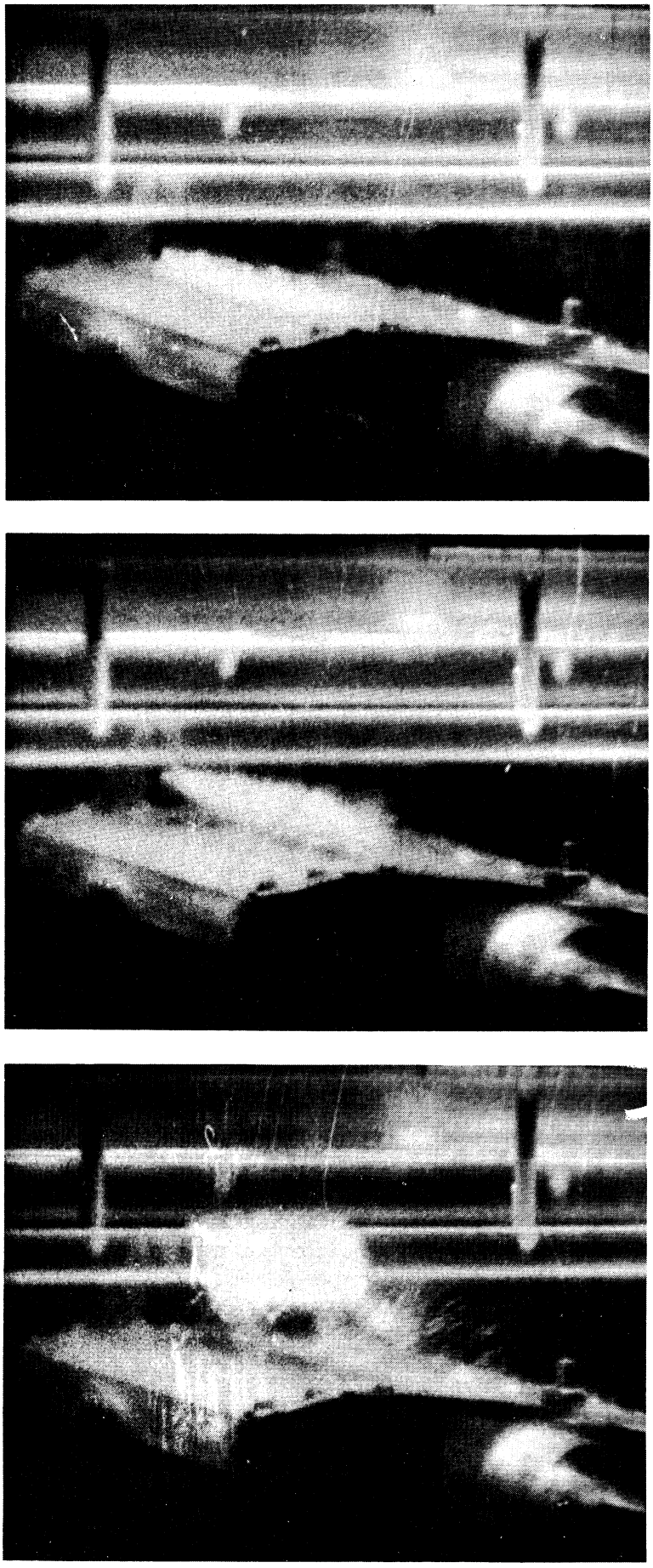

Fig. 10. Ice Removal of Heated Ice from Model in Wind Tunnel.

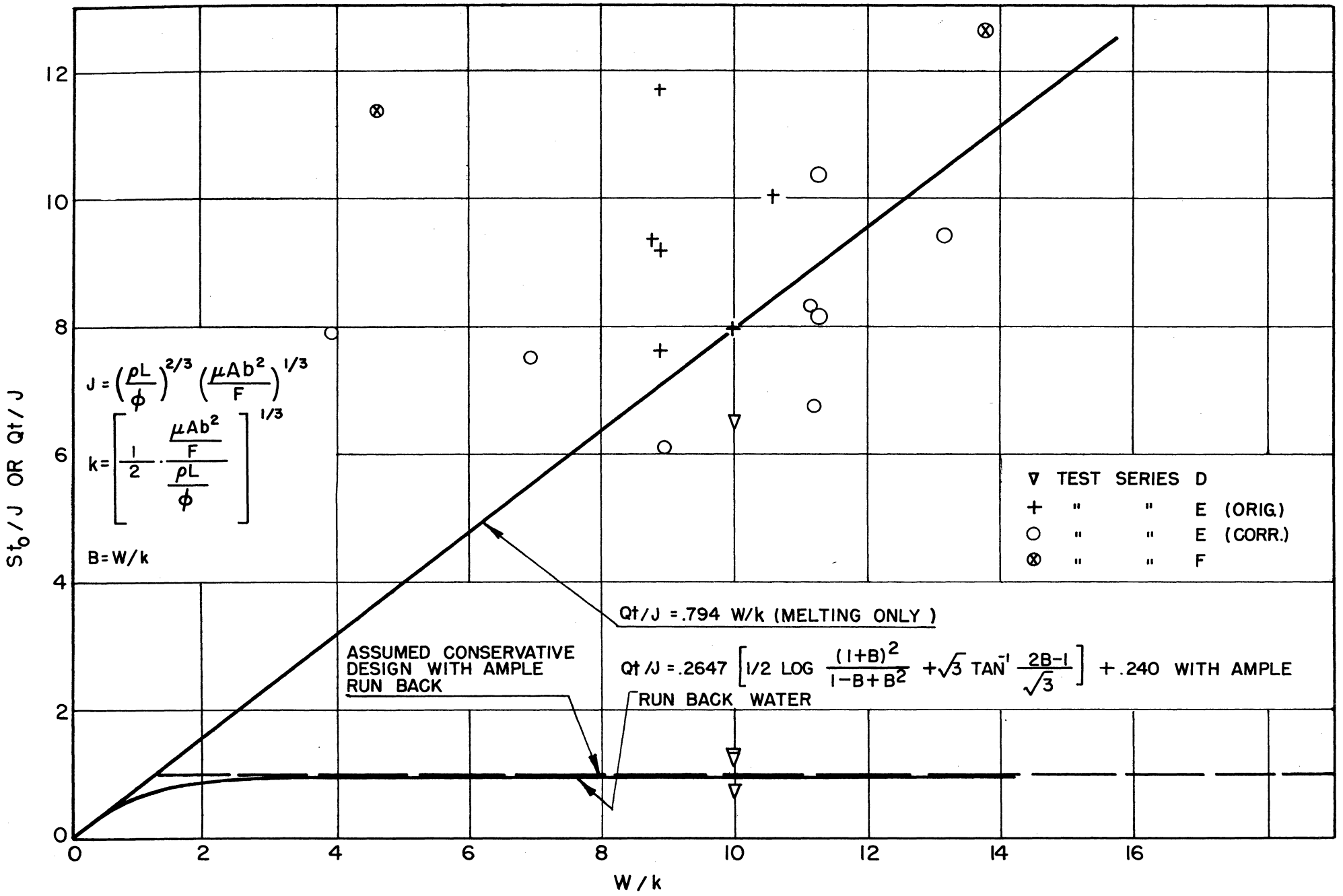

Fig. 11. Time, t, vs Water Layer Thickness W.

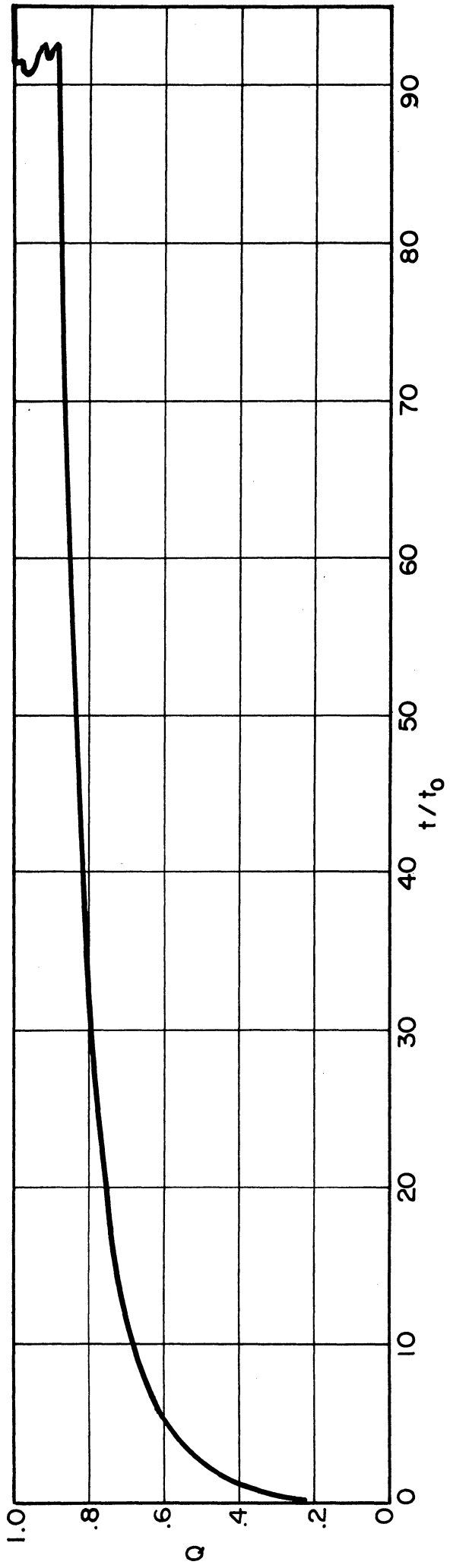

$$Q = \frac{2}{\pi} \cdot \frac{1}{t/t_0} \cdot \left[(1+t/t_0) \, \text{TAN}^{-1} \sqrt{t/t_0} - \sqrt{t/t_0} \right]$$

Fig. 12. Q vs t/t_0.

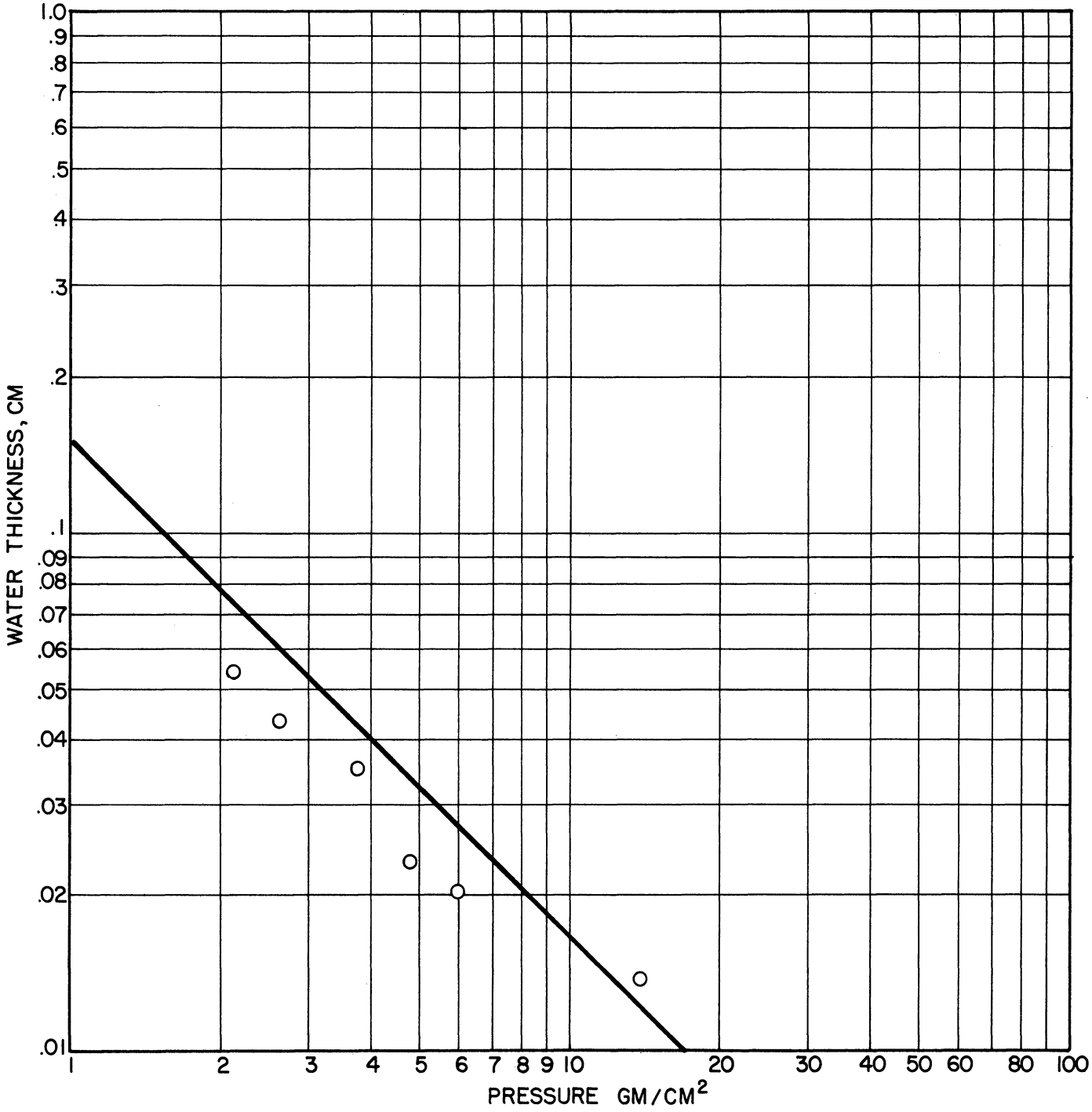

Fig. 13. Separation Force vs Water Thickness. Series A.

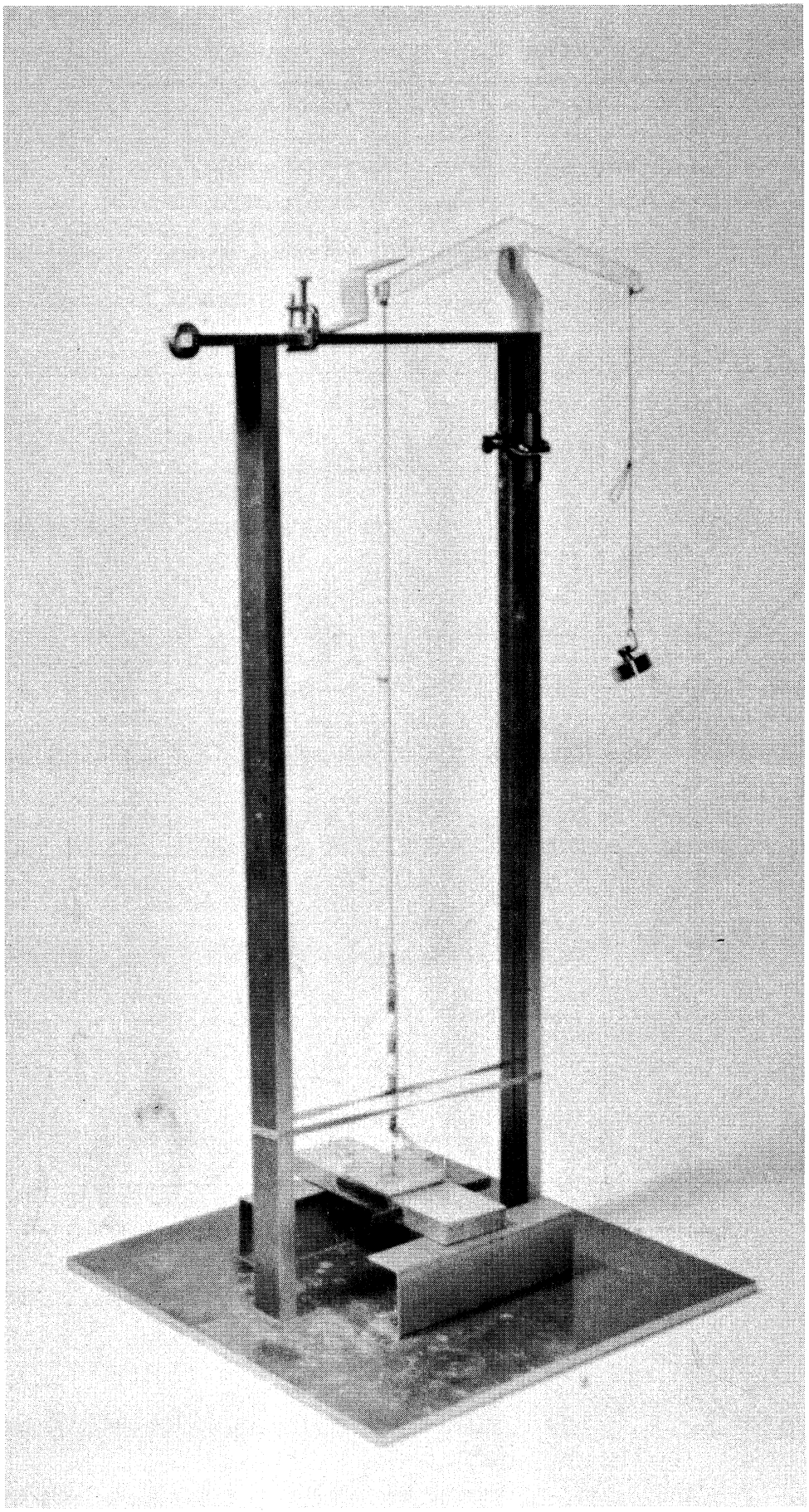

Fig. 14. Device used in Experiments of Series B.

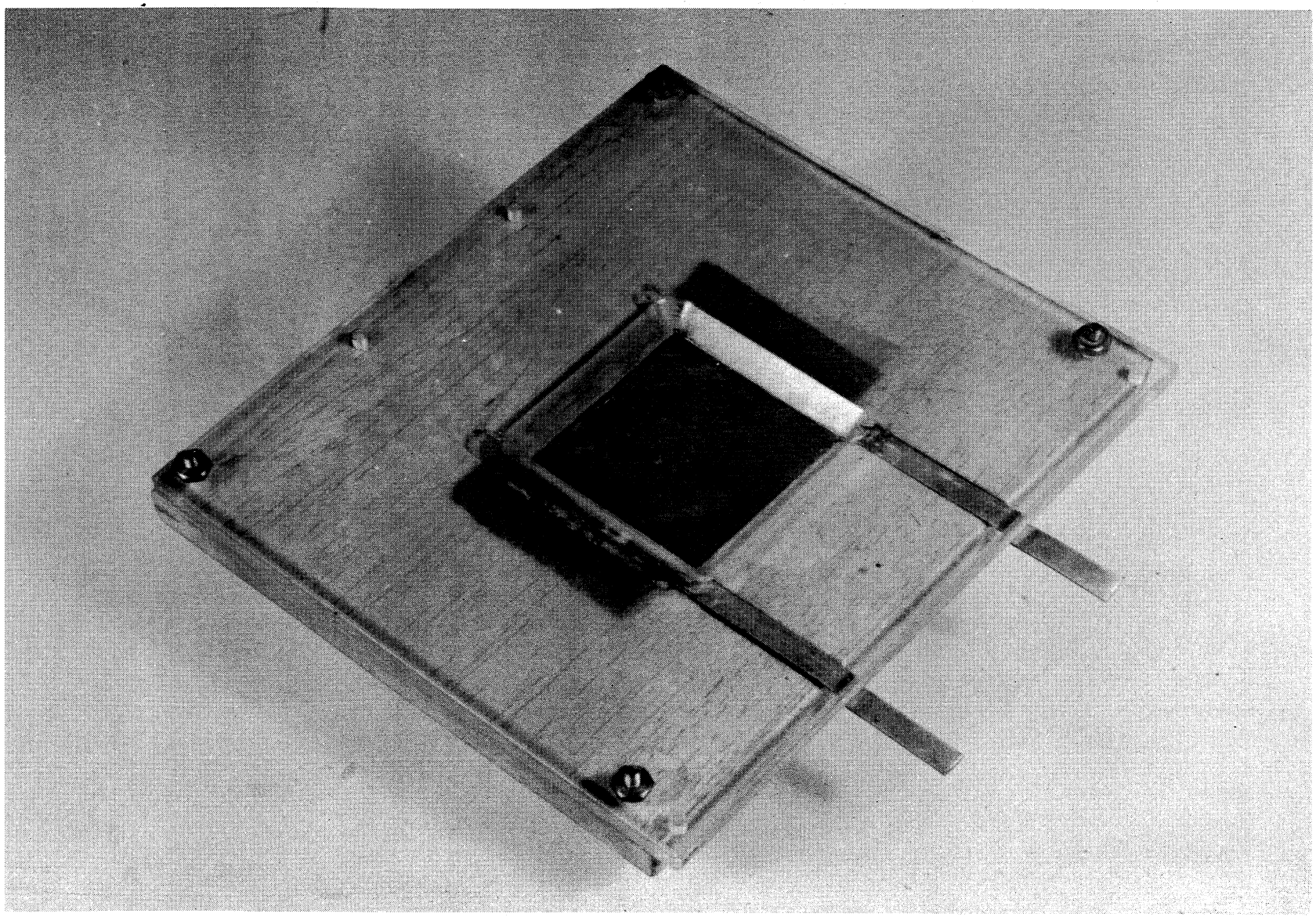

Fig. 15. Heater Element used in Excess Water Experiments. Series D.

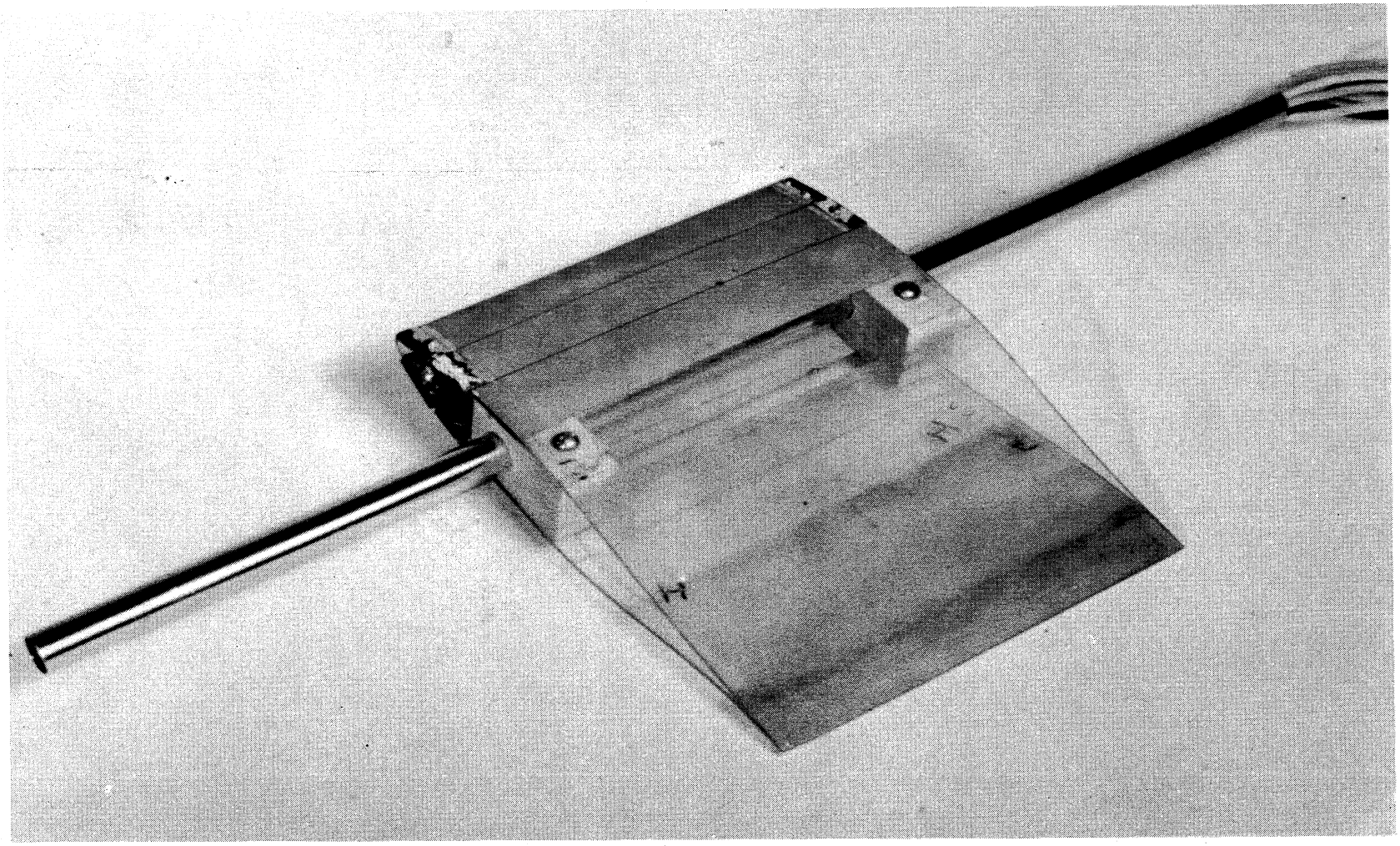

Fig. 16. Model Airfoil used in Tests of Series E Showing Printed Heater Strips.

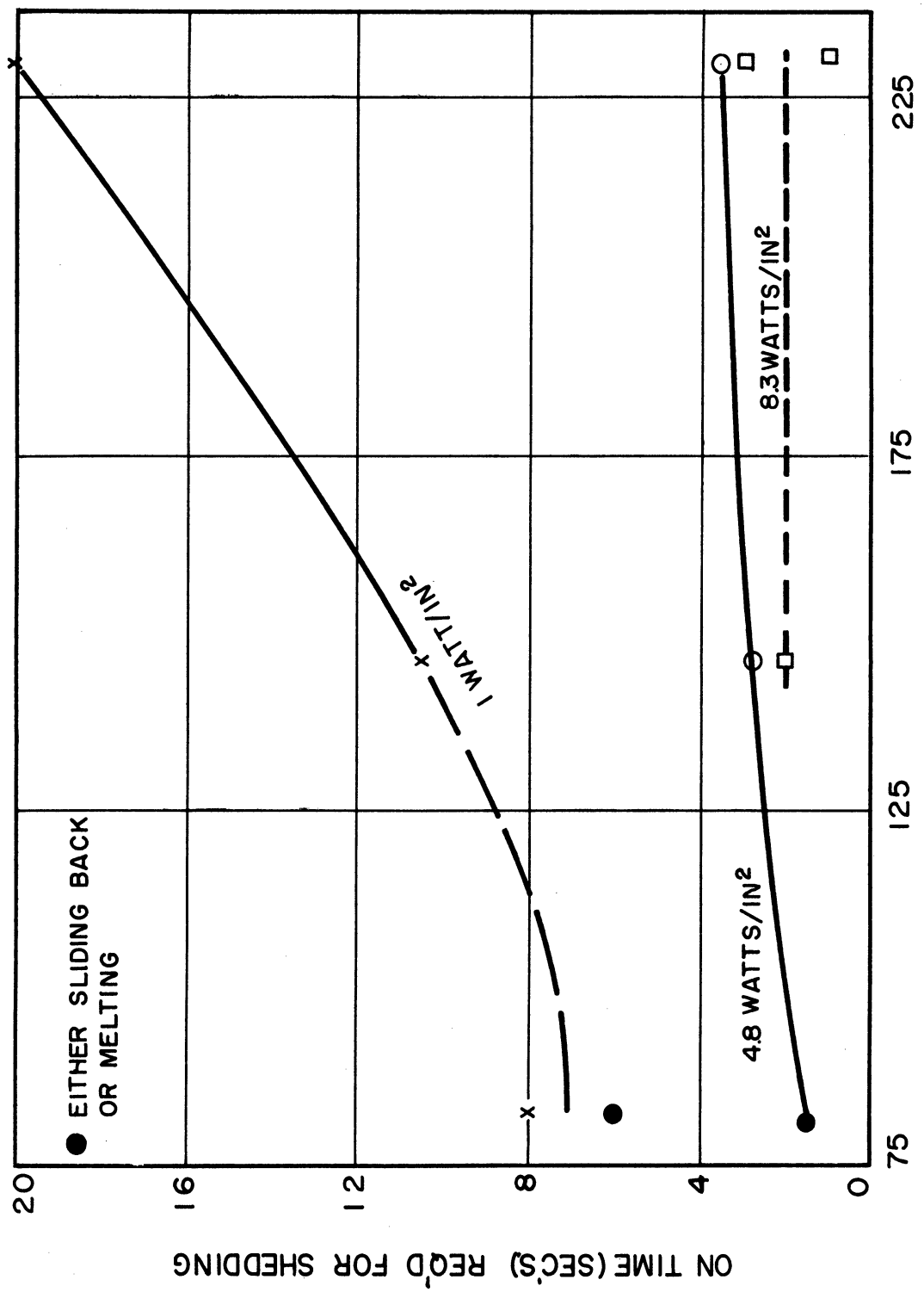

Fig. 17. Plot of On Time Required for Shedding vs Velocity for Various Power Densities.

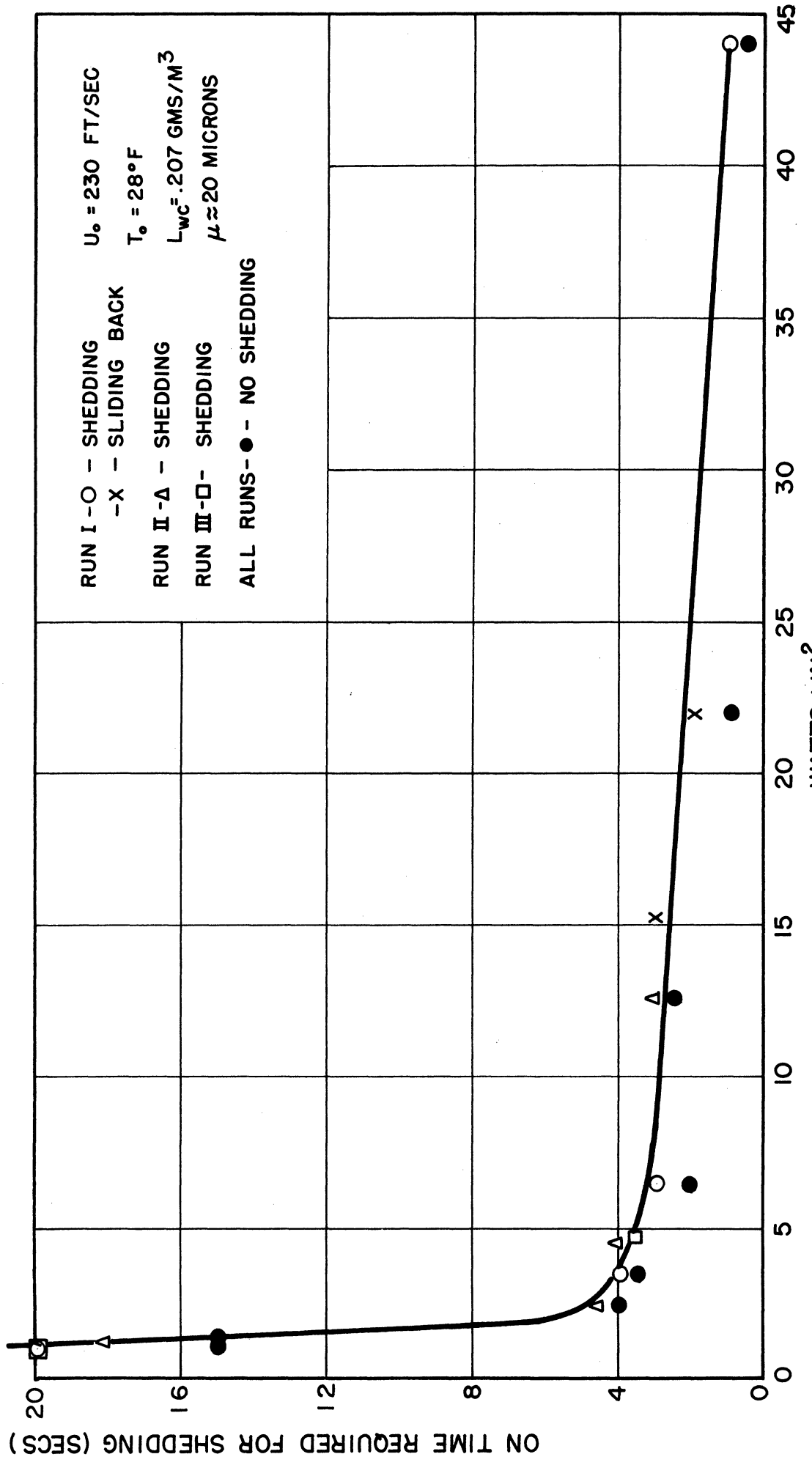

Fig. 18. Plot of Power on Time vs Power Density.

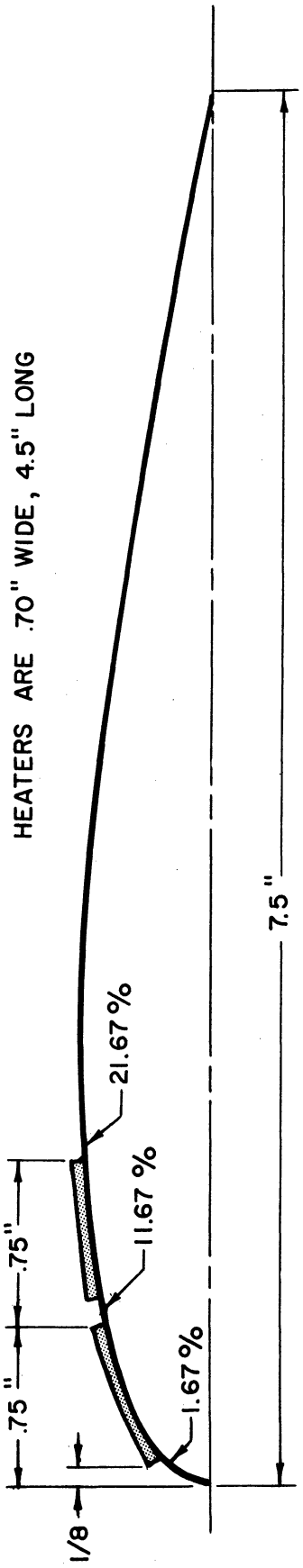

Fig. 19. NACA 65_2 - 015 Airfoil.

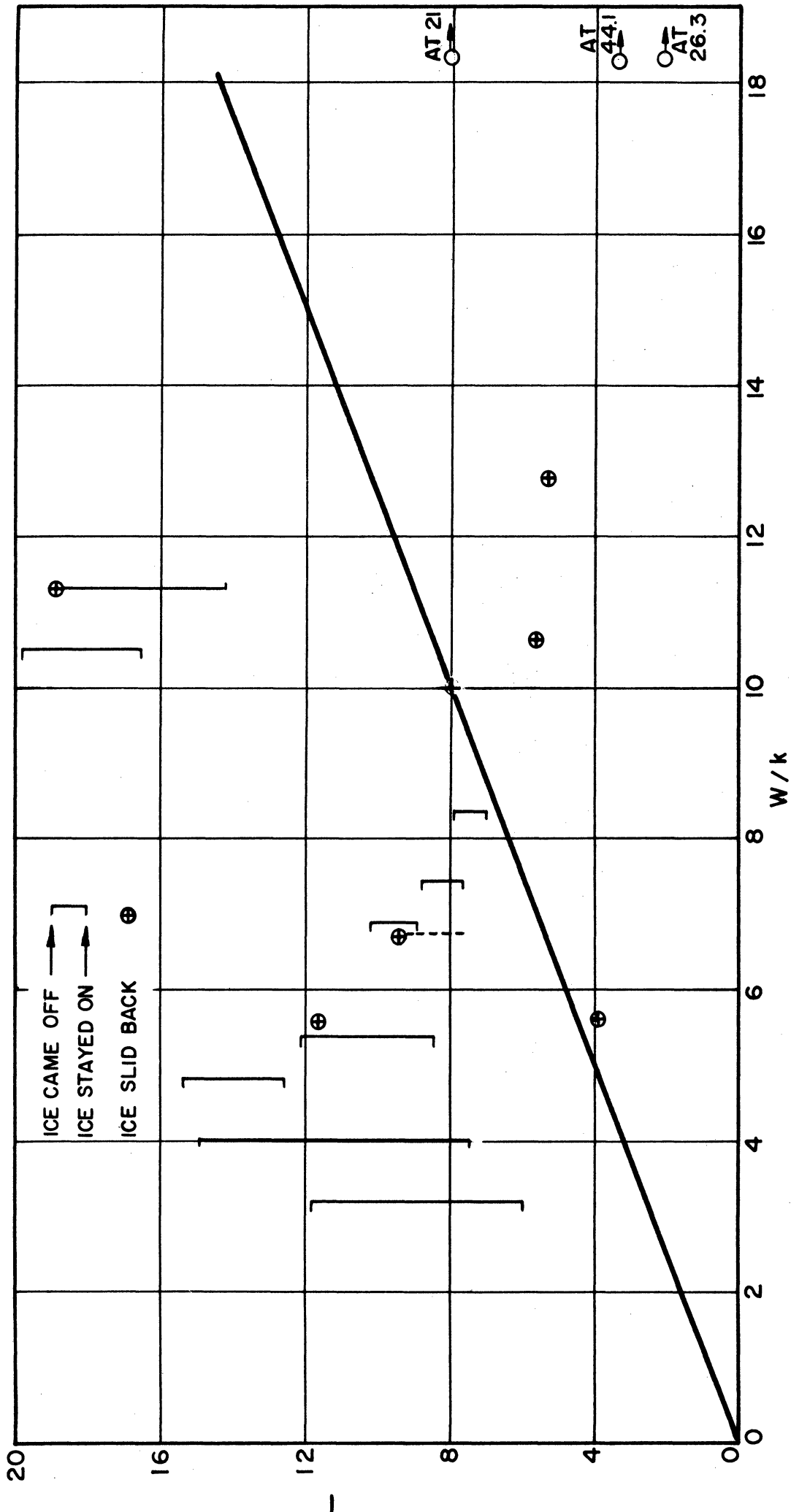

Fig. 20. Results of Wind Tunnel Tests.

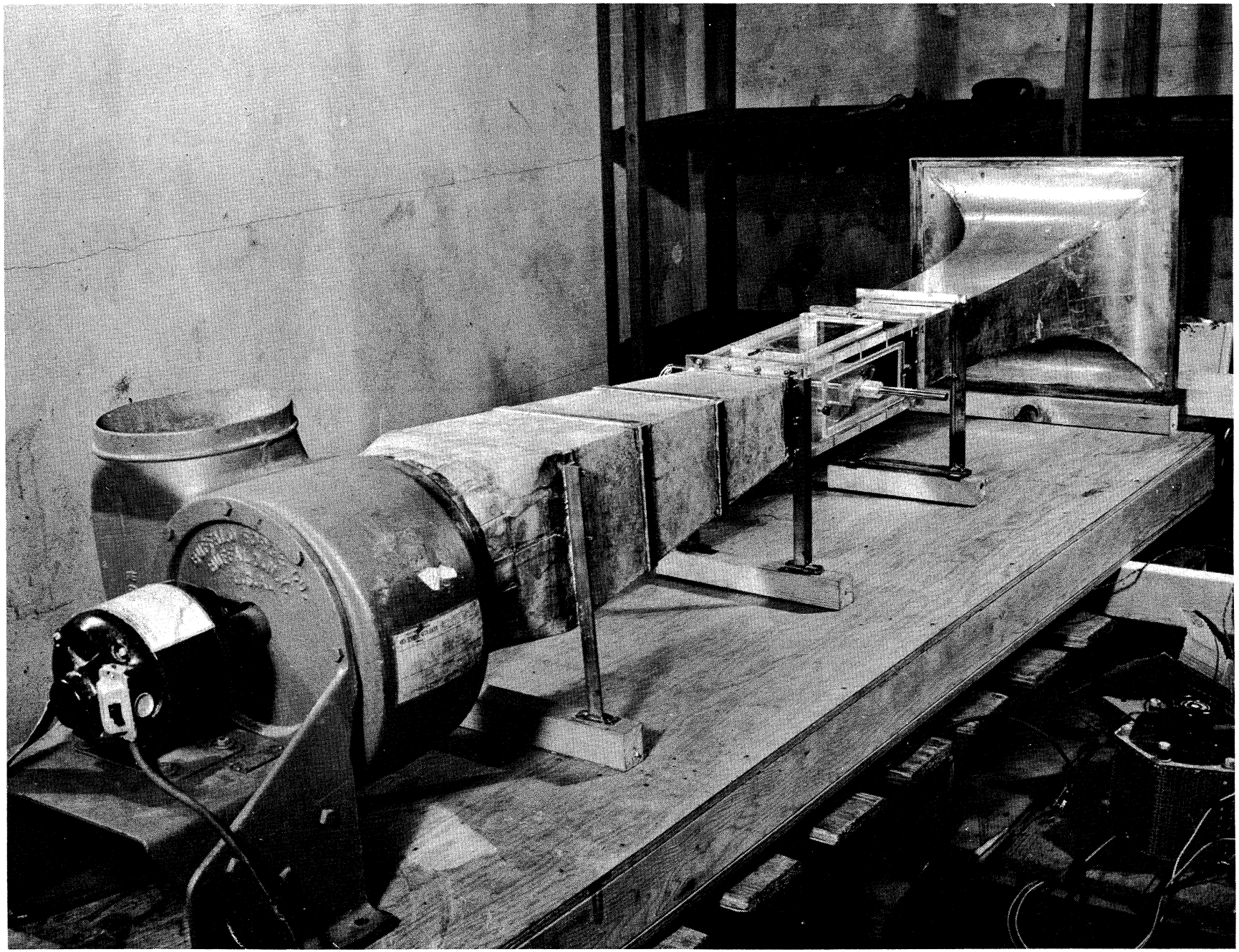

Fig. 21. View of Wind Tunnel